Low-energy reactions $K^- p \to \Sigma^0\pi^0$, $\Lambda\pi^0$, $\bar{K}^0 n$ and the strangeness $S = -1$ hyperons

Xian-Hui Zhong[1,3,*] and Qiang Zhao[2,3,†]

[1]*Department of Physics, Hunan Normal University, and Key Laboratory of Low-Dimensional Quantum Structures and Quantum Control of Ministry of Education, Changsha 410081, China*

[2]*Institute of High Energy Physics, Chinese Academy of Sciences, Beijing 100049, China*

[3]*Theoretical Physics Center for Science Facilities, Chinese Academy of Sciences, Beijing 100049, China*

(Received 27 April 2013; revised manuscript received 29 June 2013; published 29 July 2013)

A combined study of the reactions $K^- p \to \Sigma^0\pi^0$, $\Lambda\pi^0$, and $\bar{K}^0 n$ at low energies is carried out with a chiral quark-model approach. Good descriptions of the experimental observations are obtained. The roles of the low-lying strangeness $S = -1$ hyperon resonances in these processes are carefully analyzed. We find that (i) in the $K^- p \to \Sigma^0\pi^0$ process, both $\Lambda(1405)S_{01}$ and $\Lambda(1520)D_{03}$ play dominant roles. Significant contributions of $\Lambda(1670)S_{01}$ and $\Lambda(1690)D_{03}$ could be seen around their threshold; (ii) in the $K^- p \to \Lambda\pi^0$ process, some obvious evidence of $\Sigma(1775)D_{15}$ and $\Sigma(1750)S_{11}$ could be found. Some hints of $\Sigma(1620)S_{11}$ might exist in the reaction as well. $\Sigma(1750)S_{11}$ and $\Sigma(1620)S_{11}$ should correspond to the representations $[70,^4 8]S_{11}$ and $[70,^2 8]S_{11}$, respectively; (iii) in the $K^- p \to \bar{K}^0 n$ process, the dominant resonances are $\Lambda(1405)$ and $\Lambda(1520)$. Some evidence of $\Lambda(1690)D_{03}$, $\Sigma(1670)D_{13}$, and $\Sigma(1775)D_{15}$ could be seen as well. A weak coupling of $\Lambda(1670)S_{01}$ to $\bar{K}N$ should be needed in the reactions $K^- p \to \Sigma^0\pi^0$ and $\bar{K}^0 n$. Furthermore, by analyzing these reactions, we also find that the u-, t-channel backgrounds and s-channel Born term play crucial roles in the reactions: (i) The angle distributions of $K^- p \to \Sigma^0\pi^0$ are very sensitive to the u-, t-channel backgrounds and s-channel Λ pole; (ii) the reaction $K^- p \to \Lambda\pi^0$ is dominated by the u-, t-channel backgrounds and the ground P-wave state $\Sigma(1385)P_{13}$; (iii) while the reaction $K^- p \to \bar{K}^0 n$ is governed by the t-channel background, and $\Sigma(1385)P_{13}$ also plays an important role in this reaction.

DOI: 10.1103/PhysRevC.88.015208 PACS number(s): 12.39.Fe, 12.39.Jh, 13.75.Jz, 14.20.Jn

I. INTRODUCTION

There exist many puzzles in the spectroscopies of Λ and Σ hyperons. To clearly see the status of these hyperon spectroscopies, we have collected all the strangeness $S = -1$ hyperons classified in the quark model up to the $n = 2$ shell in Table I. From the table, it is seen that only a few low-lying $S = -1$ hyperons are established, while for most of them there is still no confirmed evidence found in experiments. Concretely, for the Σ spectroscopy, although a lot of states, such as those denoted by $\Sigma(1480)$"Bumps," $\Sigma(1560)$"Bumps," $\Sigma(1670)$"Bumps," and $\Sigma(1690)$"Bumps," have been listed by the Particle Data Group (PDG) [1], they are not established at all. Their quantum numbers and structures are still unknown. Even for the well-established states with known quantum numbers, such as $\Sigma(1750)1/2^-$, it is questionable in the classification of them according to various quark models [2–6]. For the Λ spectroscopy, a little more knowledge is known compared with that of Σ, however, the properties of some Λ resonances with confirmed quantum numbers are still controversial. For example, it is still undetermined whether these states, such as $\Lambda(1405)$, $\Lambda(1670)$, and $\Lambda(1520)$, are excited three quark states or dynamically generated resonances, though their J^P are well determined [3]. How to clarify these issues and extract information about the unestablished hyperon resonances from experimental data are still open questions.

To uncover the puzzles in the $S = -1$ hyperon spectroscopies, many theoretical and experimental efforts have been performed. Theoretically, (i) the mass spectroscopes were predicted in various quark models [4,5,7–14], large N_c QCD approach [13,14], and lattice QCD, etc. [15,16]; (ii) the strong decays were studied within different models [4,6,17–19]; (iii) the properties of the individual resonances, such as $\Lambda(1405)$, $\Lambda(1670)$, and $\Lambda(1520)$, were attempted to extract from the $K^- p$ scattering data with UχPT approaches [20–33], BχPT approaches [34], K-matrix methods [35,36], large-N_c QCD method [37], meson-exchange models [38–40], quark model approaches [41,42], dispersion relations [43,44], and the other hadronic models [45–48]; (iv) furthermore, the possible exotic properties of some strange baryons, such as two mesons–one baryon bound states, quark mass dependence, five-quark components, were also discussed in the literature [49–51]. Experimentally, the information of the hyperon resonances was mainly obtained from the measurements of the reactions $\bar{K}N \to \bar{K}N$, $\Sigma\pi$, $\Lambda\pi$, ηn, $\Sigma\pi\pi$, and $\Lambda\pi\pi$ [52–71]. In recent years, some other new experiments, such as excited hyperon productions from γN and NN collisions, had been carried out at LEPS, JLAB, and COSY to investigate the hyperon properties further [72–75].

Recently, some higher precision data of the reactions $K^- p \to \Sigma^0\pi^0$ [76,77], $\Lambda\pi^0$, and $\bar{K}^0 n$ [77] at eight momentum beams between 514 and 750 MeV/c were reported, which provides us a good opportunity to study these low-lying Λ and Σ resonances systemically. In this work, we carry out a combined study of these reactions in a chiral quark model, where an effective chiral Lagrangian is introduced to account for the quark-meson coupling. Since the quark-meson

*zhongxh@hunnu.edu.cn
†zhaoq@ihep.ac.cn

TABLE I. The classification of the strangeness $S = -1$ hyperons in the quark model up to $n = 2$ shell. The "?" denotes a resonance being unestablished. $l_{I,2J}$ is the PDG notation of baryons. N_6 and N_3 denote the SU(6) and SU(3) representation, respectively. **L** and **S** stand for the total orbital momentum and spin of the baryon wave function, respectively.

$[N_6, {}^{2S+1}N_3, n, \mathbf{L}]$	$l_{I,2J}$	$l_{I,2J}$
[**56**, ^{2}**8**, 0, **0**]	$P_{01}(1116)$	$P_{11}(1193)$
[**56**, ^{4}**10**, 0, **0**]	...	$P_{13}(1385)$
[**70**, ^{2}**1**, 1, **1**]	$S_{01}(1405)$	...
	$D_{03}(1520)$	...
[**70**, ^{2}**10**, 1, **1**]	...	$S_{11}(?)$
	...	$D_{13}(?)$
[**70**, ^{2}**8**, 1, **1**]	$S_{01}(1670)$	$S_{11}(?)$
	$D_{03}(1690)$	$D_{13}(1670)$
[**70**, ^{4}**8**, 1, **1**]	$S_{01}(1800)$	$S_{11}(?)$
	$D_{03}(?)$	$D_{13}(?)$
	$D_{05}(1830)$	$D_{15}(1775)$
[**56**, ^{2}**8**, 2, **0**]	$P_{01}(1600)$	$P_{11}(1660)$
[**56**, ^{2}**8**, 2, **2**]	$P_{03}(?)$	$P_{13}(?)$
	$F_{05}(?)$	$F_{15}(?)$
[**56**, ^{4}**10**, 2, **0**]	...	$P_{13}(?)$
[**56**, ^{4}**10**, 2, **2**]	...	$P_{11}(?)$
	...	$P_{13}(?)$
	...	$F_{15}(?)$
	...	$F_{17}(?)$
[**70**, ^{2}**1**, 2, **0**]	$P_{01}(1810?)$	...
[**70**, ^{2}**1**, 2, **2**]	$P_{03}(?)$	...
	$F_{05}(?)$	...
[**70**, ^{2}**10**, 2, **0**]	...	$P_{11}(?)$
[**70**, ^{2}**10**, 2, **2**]	...	$P_{13}(?)$
	...	$F_{15}(?)$
[**70**, ^{2}**8**, 2, **0**]	$P_{01}(?)$	$P_{11}(?)$
[**70**, ^{2}**8**, 2, **2**]	$P_{03}(?)$	$P_{13}(?)$
	$F_{05}(?)$	$F_{15}(?)$
[**70**, ^{4}**8**, 2, **0**]	$P_{03}(?)$	$P_{13}(?)$
[**70**, ^{4}**8**, 2, **2**]	$P_{01}(?)$	$P_{11}(?)$
	$P_{03}(?)$	$P_{13}(?)$
	$F_{05}(?)$	$F_{15}(?)$
	$F_{07}(?)$	$F_{17}(?)$

coupling is invariant under the chiral transformation, some of the low-energy properties of QCD are retained. The chiral quark model has been well developed and widely applied to meson photoproduction reactions [78–88]. Its recent extension to describe the process of πN [89] and $\bar{K}N$ [42] scattering, and the charmed hadron strong decays [90–92] also turns out to be successful and inspiring.

This work is organized as follows. In Sec. II, the formulism of the model is reviewed. Then, the partial wave amplitudes are separated in Sec. III. The numerical results are presented and discussed in Sec. IV. Finally, a summary is given in Sec. V.

II. FRAMEWORK

The tree diagrams calculated in the chiral quark model have been shown in Fig. 1. The reaction amplitude can be expressed

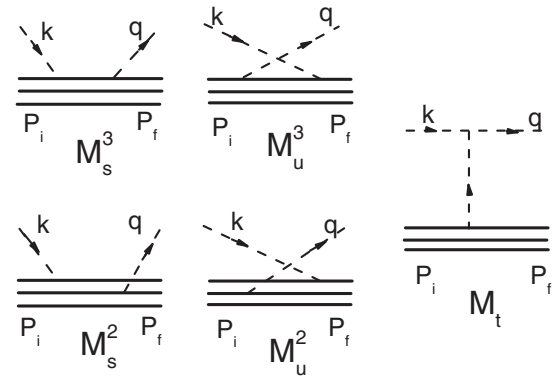

FIG. 1. s, u, and t channels are considered in this work. M_s^3 and M_u^3 (M_s^2, M_u^2) correspond to the amplitudes of s and u channels for the incoming and outgoing mesons absorbed and emitted by the same quark (different quarks), respectively.

as the sum of the s-, u-, t-channel transition amplitudes:

$$\mathcal{M} = \mathcal{M}_s + \mathcal{M}_u + \mathcal{M}_t. \tag{1}$$

The s- and u-channel transition amplitudes as shown in Fig. 1 are given by

$$\mathcal{M}_s = \sum_j \langle N_f | H_m^f | N_j \rangle \langle N_j | \frac{1}{E_i + \omega_i - E_j} H_m^i | N_i \rangle, \tag{2}$$

$$\mathcal{M}_u = \sum_j \langle N_f | H_m^i \frac{1}{E_i - \omega_f - E_j} | N_j \rangle \langle N_j | H_m^f | N_i \rangle, \tag{3}$$

where H_m^i and H_m^f stand for the incoming and outgoing meson-quark couplings, which might be described by the effective chiral Lagrangian [86,87],

$$H_m = \frac{1}{f_m} \bar{\psi}_j \gamma_\mu^j \gamma_5^j \psi_j \vec{\tau} \cdot \partial^\mu \vec{\phi}_m, \tag{4}$$

where ψ_j represents the jth quark field in a hadron, and f_m is the meson's decay constant. The pseudoscalar-meson octet, ϕ_m, is written as

$$\phi_m = \begin{pmatrix} \frac{1}{\sqrt{2}}\pi^0 + \frac{1}{\sqrt{6}}\eta & \pi^+ & K^+ \\ \pi^- & -\frac{1}{\sqrt{2}}\pi^0 + \frac{1}{\sqrt{6}}\eta & K^0 \\ K^- & \bar{K}^0 & -\sqrt{\frac{2}{3}}\eta \end{pmatrix}. \tag{5}$$

In Eqs. (2) and (3), ω_i and ω_f are the energies of the incoming and outgoing mesons, respectively. $|N_i\rangle$, $|N_j\rangle$, and $|N_f\rangle$ stand for the initial, intermediate, and final states, respectively, and their corresponding energies are E_i, E_j, and E_f, which are the eigenvalues of the nonrelativistic Hamiltonian of the constituent quark model $\hat{H}$ [5,7].

The extracted transition amplitude for the s channel is [42,89]

$$\begin{aligned}\mathcal{M}_s = &\left\{ \sum_{n=0} \left(g_{s1} + \frac{1}{(-2)^n} g_{s2} \right) \mathbf{A}_{\text{out}} \cdot \mathbf{A}_{\text{in}} \frac{F_s(n)}{n!} \mathcal{X}^n \right. \\ &+ \sum_{n=1} \left(g_{s1} + \frac{1}{(-2)^n} g_{s2} \right) \frac{F_s(n)}{(n-1)!} \mathcal{X}^{n-1} \\ &\times \left. \left(\frac{\omega_i}{6\mu_q} \mathbf{A}_{\text{out}} \cdot \mathbf{q} + \frac{\omega_i}{3m_q} \mathbf{A}_{\text{in}} \cdot \mathbf{k} + \frac{\omega_i}{m_q} \frac{\omega_i}{2\mu_q} \alpha^2 \right) \right.\end{aligned}$$

$$+\sum_{n=2}\left(g_{s1}+\frac{1}{(-2)^n}g_{s2}\right)\frac{\omega_f\omega_i}{18m_q\mu_q}\mathbf{k}\cdot\mathbf{q}\frac{F_s(n)}{(n-2)!}\mathcal{X}^{n-2}$$
$$+\sum_{n=0}\left(g_{v1}+\frac{1}{(-2)^n}g_{v2}\right)i\boldsymbol{\sigma}\cdot(\mathbf{A}_{\rm out}\times\mathbf{A}_{\rm in})\frac{F_s(n)}{n!}\mathcal{X}^n$$
$$-\sum_{n=2}\left(g_{v1}+\frac{1}{(-2)^n}g_{v2}\right)\frac{\omega_f\omega_i}{18m_q\mu_q}i\boldsymbol{\sigma}\cdot(\mathbf{q}\times\mathbf{k})$$
$$\times\frac{F_s(n)}{(n-2)!}\mathcal{X}^{n-2}\Bigg\}e^{-(\mathbf{k}^2+\mathbf{q}^2)/6\alpha^2}, \quad (6)$$

with

$$\mathbf{A}_{\rm in}=-\left(\omega_i\mathcal{K}_i+\frac{\omega_i}{6\mu_q}+1\right)\mathbf{k}, \quad (7)$$
$$\mathbf{A}_{\rm out}=-\left(\omega_f\mathcal{K}_f+\frac{\omega_f}{6\mu_q}+1\right)\mathbf{q}, \quad (8)$$

where $\mathcal{K}_i\equiv 1/(E_i+M_i)$, $\mathcal{K}_f\equiv 1/(E_f+M_f)$, and m_q is the light quark mass. The $\mathcal{X}$ is defined as $\mathcal{X}\equiv\mathbf{k}\cdot\mathbf{q}/(3\alpha^2)$, and the factor $F_s(n)$ is given by expanding the energy propagator in Eq. (6) which leads to

$$F_s(n)=\frac{M_n}{P_i\cdot k-nM_n\omega_h}, \quad (9)$$

where M_n is the mass of the intermediate baryons in the nth shell, while ω_h is the typical energy of the harmonic oscillator; P_i and k are the four momenta of the initial baryons and incoming mesons in the center-of-mass (c.m.) system, respectively.

While the extracted transition amplitude for the u channel is [42,89]

$$\mathcal{M}_u=-\Bigg\{\mathbf{B}_{\rm in}\cdot\mathbf{B}_{\rm out}\sum_{n=0}\left[g^u_{s1}+(-2)^{-n}g^u_{s2}\right]\frac{F_u(n)}{n!}\mathcal{X}^n$$
$$+\left(\frac{\omega_f}{3m_q}\mathbf{B}_{\rm in}\cdot\mathbf{k}+\frac{\omega_i}{6\mu_q}\mathbf{B}_{\rm out}\cdot\mathbf{q}+\frac{\omega_i}{2\mu_q}\frac{\omega_f}{m_q}\alpha^2\right)$$
$$\times\sum_{n=1}\left[g^u_{s1}+(-2)^{-n}g^u_{s2}\right]\frac{F_u(n)}{(n-1)!}\mathcal{X}^{n-1}$$
$$+\frac{\omega_f\omega_i}{18m_q\mu_q}\mathbf{k}\cdot\mathbf{q}\sum_{n=2}\frac{F_u(n)}{(n-2)!}\left[g^u_{s1}+(-2)^{-n}g^u_{s2}\right]\mathcal{X}^{n-2}$$
$$+i\boldsymbol{\sigma}\cdot(\mathbf{B}_{\rm in}\times\mathbf{B}_{\rm out})\sum_{n=0}\left[g^u_{v1}+(-2)^{-n}g^u_{v2}\right]\frac{F_u(n)}{n!}\mathcal{X}^n$$
$$+\frac{\omega_f\omega_i}{18m_q\mu_q}i\boldsymbol{\sigma}\cdot(\mathbf{q}\times\mathbf{k})\sum_{n=2}\left[g^u_{v1}+(-2)^{-n}g^u_{v2}\right]\mathcal{X}^{n-2}$$
$$\times\frac{F_u(n)}{(n-2)!}+i\boldsymbol{\sigma}\cdot\left[\frac{\omega_f}{3m_q}(\mathbf{B}_{\rm in}\times\mathbf{k})+\frac{\omega_i}{6\mu_q}(\mathbf{q}\times\mathbf{B}_{\rm out})\right]$$
$$\times\sum_{n=1}\left[g^u_{v1}+(-2)^{-n}g^u_{v2}\right]\mathcal{X}^{n-1}\frac{F_u(n)}{(n-1)!}\Bigg\}$$
$$\times e^{-(\mathbf{k}^2+\mathbf{q}^2)/6\alpha^2}, \quad (10)$$

where we have defined

$$\mathbf{B}_{\rm in}\equiv-\omega_i\left(K_f+K_j+\frac{1}{6\mu_q}\right)\mathbf{q}-(\omega_iK_j+1)\mathbf{k}, \quad (11)$$
$$\mathbf{B}_{\rm out}\equiv-\omega_f\left(K_i+K_j+\frac{1}{6\mu_q}\right)\mathbf{k}-(\omega_fK_j+1)\mathbf{q}, \quad (12)$$

with $\mathcal{K}_j\equiv 1/(E_j+M_j)$. The factor $F_u(n)$ is given by

$$F_u(n)=\frac{M_n}{P_i\cdot q+nM_n\omega_h}, \quad (13)$$

where q stands for the four momenta of the outgoing mesons in the c.m. system.

The g factors appearing in the s- and u-channel amplitudes are determined by [42]

$$g_{s1}\equiv\langle N_f|\sum_j I^f_jI^i_j|N_i\rangle/3, \quad (14)$$
$$g_{s2}\equiv\langle N_f|\sum_{i\neq j} I^f_iI^i_j\boldsymbol{\sigma}_i\cdot\boldsymbol{\sigma}_j|N_i\rangle/3, \quad (15)$$
$$g_{v1}\equiv\langle N_f|\sum_j I^f_iI^i_j\boldsymbol{\sigma}_{jz}|N_i\rangle/2, \quad (16)$$
$$g_{v2}\equiv\langle N_f|\sum_{i\neq j} I^f_iI^i_j(\boldsymbol{\sigma}_i\times\boldsymbol{\sigma}_j)_z|N_i\rangle/2, \quad (17)$$
$$g^u_{s1}\equiv\langle N_f|\sum_j I^i_jI^f_j|N_i\rangle, \quad (18)$$
$$g^u_{s2}\equiv\langle N_f|\sum_{i\neq j} I^i_iI^f_j\boldsymbol{\sigma}_i\cdot\boldsymbol{\sigma}_j|N_i\rangle/3, \quad (19)$$
$$g^u_{v1}\equiv\langle N_f|\sum_j I^i_jI^f_j\sigma^z_j|N_i\rangle, \quad (20)$$
$$g^u_{v2}\equiv\langle N_f|\sum_{i\neq j} I^i_iI^f_j(\boldsymbol{\sigma}_i\times\boldsymbol{\sigma}_j)_z|N_i\rangle/2, \quad (21)$$

where $\boldsymbol{\sigma}_j$ corresponds to the Pauli spin vector of the jth quark in a hadron, I^i_j and I^f_j are the isospin operators of the initial and final mesons defined in [42].

These g factors can be derived in the SU(6)⊗O(3) symmetry limit. In Table II, we have listed the g factors for the reactions $K^-p\to\Sigma^0\pi^0$, $\Lambda\pi^0$, and $\bar{K}^0n$. From these factors, we can see some interesting features of these reactions. For example, it is found that in the reactions $K^-p\to\Sigma^0\pi^0$ and $\Lambda\pi^0$, the K^- and π^0 mesons cannot couple to the same quark of an s-channel intermediate state (i.e., $g_{s1}=g_{v1}=0$), which leads to a strong suppression of the s-channel contributions. However, for the u channel the kaon and pion can couple to not only the same quark but also different quarks of a baryon. Thus, the u channel could contribute a large background to these two processes. While for the charge-exchange reaction $K^-p\to\bar{K}^0n$, there are no u-channel contributions (i.e., $g^u=0$), and only the s-channel amplitude M^s_3 survives for the isospin selection rule (i.e., $g_{s2}=g_{v2}=0$).

In this work, we consider the vector exchange and the scalar exchange for the t-channel backgrounds. The vector

TABLE II. Various g and g_R factors extracted in the symmetric quark model.

$K^-p \to \Sigma^0\pi^0$		$K^-p \to \Lambda\pi^0$		$K^-p \to \bar{K}^0 n$	
Factor	Value	Factor	Value	Factor	Value
g^u_{s1}	1/2	g^u_{s1}	$\sqrt{3}/2$	g_{s1}	1
g^u_{s2}	1	g^u_{s2}	$\sqrt{3}/3$	g_{v1}	5/3
g^u_{v1}	$-1/6$	g^u_{v1}	$\sqrt{3}/2$	$g_{S_{01}[70,^21]}$	27/36
g^u_{v2}	-1	g^u_{v2}	$\sqrt{3}/3$	$g_{S_{01}[70,^28]}$	27/36
g_{s2}	1	g_{s2}	$\sqrt{3}/3$	$g_{S_{11}[70,^28]}$	$-1/36$
g_{v2}	1	g_{v2}	$-\sqrt{3}/3$	$g_{S_{11}[70,^48]}$	$-16/36$
$g_{S_{01}[70,^21]}$	3/2	$g_{S_{11}[70,^28]}$	$-1/6$	$g_{S_{11}[70,^210]}$	$-1/36$
$g_{S_{01}[70,^28]}$	$-1/2$	$g_{S_{11}[70,^48]}$	4/6	$g_{D_{03}[70,^21]}$	135/252
$g_{D_{03}[70,^21]}$	3/2	$g_{S_{11}[70,^210]}$	$-1/6$	$g_{D_{03}[70,^28]}$	135/252
$g_{D_{03}[70,^28]}$	$-1/2$	$g_{D_{13}[70,^28]}$	5/6	$g_{D_{13}[70,^28]}$	$-5/252$
		$g_{D_{13}[70,^48]}$	$-4/6$	$g_{D_{13}[70,^48]}$	$-8/252$
		$g_{D_{13}[70,^210]}$	$-5/6$	$g_{D_{13}[70,^210]}$	$-5/252$
				g_Λ	27/26
				g_Σ	$-1/26$

meson-quark and scalar meson-quark couplings are given by

$$H_V = \bar{\psi}_j\left(a\gamma^\nu + \frac{b\sigma^{\nu\lambda}\partial_\lambda}{2m_q}\right)V_\nu\psi_j, \tag{22}$$

$$H_S = g_{Sqq}\bar{\psi}_j\psi_j S, \tag{23}$$

where V and S stands for the vector and scalar fields, respectively. The constants a, b, and g_{Sqq} are the vector, tensor, and scalar coupling constants, respectively. They are treated as free parameters in this work.

On the other hand, the VPP and SPP couplings (P stands for a pseudoscalar meson) are adopted as [93,94]

$$H_{\rm VPP} = -iG_V{\rm Tr}([\phi_m, \partial_\mu\phi_m]V^\mu), \tag{24}$$

$$H_{\rm SPP} = \frac{g_{\rm SPP}}{2m_\pi}\partial_\mu\phi_m\partial^\mu\phi_m S, \tag{25}$$

where G_V is the coupling constant to be determined by experimental data.

For the case of the vector meson exchange, the t-channel amplitude in the quark model is given by

$$\mathcal{M}^V_t = \mathcal{O}^t_V\frac{1}{t-M_V^2}e^{-(\mathbf{q}-\mathbf{k})^2/(6\alpha^2)}, \tag{26}$$

where $e^{-(\mathbf{q}-\mathbf{k})^2/(6\alpha^2)}$ is a form factor deduced from the quark model, and M_V is the vector-meson mass. The amplitude $\mathcal{O}^t_V$ is given by

$$\mathcal{O}^t_V = G_v a\left[g^s_t(\mathcal{H}_0 + \mathcal{H}_1\mathbf{q}\cdot\mathbf{k}) + g^v_t\mathcal{H}_2 i\boldsymbol{\sigma}\cdot(\mathbf{q}\times\mathbf{k})\right] + \text{tensor term}, \tag{27}$$

where we have defined

$$\mathcal{H}_0 \equiv E_0\left(1 + \frac{\mathcal{K}_f}{6\mu_q}\mathbf{q}^2 - \frac{\mathcal{K}_i}{6\mu_q}\mathbf{k}^2 + \frac{1}{4\mu_q^2}\left[\frac{\alpha^2}{3} + \frac{1}{9}(\mathbf{q}^2+\mathbf{k}^2)\right]\right) + \frac{1}{3\mu_q}(\mathbf{q}^2-\mathbf{k}^2) + \mathcal{K}_f\mathbf{q}^2 + \mathcal{K}_i\mathbf{k}^2, \tag{28}$$

$$\mathcal{H}_1 \equiv E_0\left[\mathcal{K}_i\mathcal{K}_f - \frac{\mathcal{K}_f}{6\mu_q} + \frac{\mathcal{K}_i}{6\mu_q} - \frac{1}{2\mu_q^2}\right] + \mathcal{K}_f + \mathcal{K}_i, \tag{29}$$

$$\mathcal{H}_2 \equiv E_0\left[\mathcal{K}_f\mathcal{K}_i - \frac{\mathcal{K}_f}{6\mu_q} + \frac{\mathcal{K}_i}{6\mu_q}\right] + \mathcal{K}_i + \mathcal{K}_f, \tag{30}$$

with $E_0 = \omega_i + \omega_f$. The tensor term of the t-channel vector-exchange amplitude is less important than that of the vector term. In the calculations, we find the results are insensitive to the tensor term, thus, its contributions are neglected for simplicity. In Eq. (27), we have defined $g^s_t \equiv \langle N_f|\sum_{j=1}^3 I^{\rm ex}_j|N_i\rangle$, and $g^v_t \equiv \langle N_f|\sum_{j=1}^3\sigma_j I^{\rm ex}_j|N_i\rangle$, which can be deduced from the quark model, where $I^{\rm ex}_j$ is the isospin operator of exchanged meson. For the $K^-p \to \Sigma^0\pi^0$, $\Lambda\pi^0$ processes, the vector K^{*+} exchange is considered, and for the $K^-p \to n\bar{K}^0$ process, the vector ρ^+ exchange is considered.

For the case of the scalar meson exchange, the t-channel amplitude in the quark model is written as

$$\mathcal{M}^S_t = \mathcal{O}^t_S\frac{1}{t-m_S^2}e^{-(\mathbf{q}-\mathbf{k})^2/(6\alpha^2)}, \tag{31}$$

where m_S is the scalar-meson mass, and the $\mathcal{O}^t_S$ is given by

$$\mathcal{O}^t_S \simeq \frac{g_{SPP}g_{Sqq}}{2m_\pi}(\omega_i\omega_f - \mathbf{q}\cdot\mathbf{k})\left[g^s_t(\mathcal{A}_0 + \mathcal{A}_1\mathbf{q}\cdot\mathbf{k}) + g^v_t\mathcal{A}_2 i\boldsymbol{\sigma}\cdot(\mathbf{q}\times\mathbf{k})\right], \tag{32}$$

with

$$\mathcal{A}_0 \equiv 1 - \frac{\mathcal{K}_f}{6\mu_q}\mathbf{q}^2 + \frac{\mathcal{K}_i}{6\mu_q}\mathbf{k}^2 - \frac{1}{4\mu_q^2}\left[\frac{\alpha^2}{3} + \frac{\mathbf{q}^2+\mathbf{k}^2}{9}\right], \tag{33}$$

$$\mathcal{A}_1 \equiv -\mathcal{K}_i\mathcal{K}_f + \frac{1}{6\mu_q}\mathcal{K}_f - \frac{1}{6\mu_q}\mathcal{K}_i + \frac{1}{18\mu_q^2}, \tag{34}$$

$$\mathcal{A}_2 \equiv -\mathcal{K}_i\mathcal{K}_f + \frac{1}{6\mu_q}\mathcal{K}_f - \frac{1}{6\mu_q}\mathcal{K}_i. \tag{35}$$

In Eq. (32), we have neglected the higher order terms. In this work, the scalar κ exchange is considered for the $K^-p \to \Sigma^0\pi^0$, $\Lambda\pi^0$ processes, while the scalar $a_0(980)$ exchange is considered for the $K^-p \to n\bar{K}^0$ process.

III. SEPARATION OF THE RESONANCE CONTRIBUTIONS

It should be noted that the amplitudes in terms of the harmonic oscillator principal quantum number n are the sum of a set of SU(6) multiplets with the same n. To see the contributions of an individual resonance listed in Table I, we need to separate out the single-resonance-excitation amplitudes within each principal number n in the s channel.

We have noticed that the transition amplitude has a unified form [95]:

$$\mathcal{O} = f(\theta) + ig(\theta)\boldsymbol{\sigma}\cdot\mathbf{n}, \tag{36}$$

where $\mathbf{n} \equiv \mathbf{q}\times\mathbf{k}/|\mathbf{k}\times\mathbf{q}|$. The non-spin-flip and spin-flip amplitudes $f(\theta)$ and $g(\theta)$ can be expanded in terms of the familiar partial wave amplitudes $T_{l\pm}$ for the states with

$J = l \pm 1/2$:

$$f(\theta) = \sum_{l=0}^{\infty}[(l+1)T_{l+} + lT_{l-}]P_l(\cos\theta), \tag{37}$$

$$g(\theta) = \sum_{l=0}^{\infty}[T_{l-} - T_{l+}]\sin\theta P_l'(\cos\theta). \tag{38}$$

Combining Eqs. (37) and (38), first, we can separate out the partial waves with different l in the same n. For example, in the $n = 0$ shell, only the P ($l = 1$) wave contributes to the reaction; in the $n = 1$ shell, both S ($l = 0$) and D ($l = 2$) waves contribute to the reaction; and in the $n = 2$ shell, only the P and F waves are involved in the process. The separated partial amplitudes, $\mathcal{O}_n(l)$, up to the $n = 2$ shell are given by [42,89]

$$\mathcal{O}_0(P) = (g_{s1} + g_{s2})\mathbf{A}_{\rm out}\cdot\mathbf{A}_{\rm in} + (g_{v1} + g_{v2})i\boldsymbol{\sigma}\cdot(\mathbf{A}_{\rm out}\times\mathbf{A}_{\rm in}), \tag{39}$$

$$\mathcal{O}_1(S) = \left(g_{s1} - \frac{1}{2}g_{s2}\right)\left(|\mathbf{A}_{\rm out}|\cdot|\mathbf{A}_{\rm in}|\frac{|\mathbf{k}||\mathbf{q}|}{9\alpha^2} + \frac{\omega_i}{6\mu_q}\mathbf{A}_{\rm out}\cdot\mathbf{q} + \frac{\omega_f}{6\mu_q}\mathbf{A}_{\rm in}\cdot\mathbf{k} + \frac{\omega_i\omega_f}{4\mu_q\mu_q}\alpha^2\right), \tag{40}$$

$$\mathcal{O}_1(D) = \left(g_{s1} - \frac{1}{2}g_{s2}\right)|\mathbf{A}_{\rm out}|\cdot|\mathbf{A}_{\rm in}|(3\cos^2\theta - 1)\frac{|\mathbf{k}||\mathbf{q}|}{9\alpha^2} + \left(g_{v1} - \frac{1}{2}g_{v2}\right)i\boldsymbol{\sigma}\cdot(\mathbf{A}_{\rm out}\times\mathbf{A}_{\rm in})\frac{\mathbf{k}\cdot\mathbf{q}}{3\alpha^2}, \tag{41}$$

$$\mathcal{O}_2(P) = \left(g_{s1} + \frac{1}{4}g_{s2}\right)\left(|\mathbf{A}_{\rm out}||\mathbf{A}_{\rm in}|\frac{|\mathbf{k}||\mathbf{q}|}{10\alpha^2} + \frac{\omega_i}{6\mu_q}\mathbf{A}_{\rm out}\cdot\mathbf{q} + \frac{\omega_f}{6\mu_q}\mathbf{A}_{\rm in}\cdot\mathbf{k} + \frac{\omega_f}{\mu_q}\frac{\omega_i}{\mu_q}\frac{\alpha^2}{3}\right)\frac{|\mathbf{k}||\mathbf{q}|}{3\alpha^2}\cos\theta - \left(g_{v1} + \frac{1}{4}g_{v2}\right)\frac{\omega_f\omega_i}{(6\mu_q)^2}i\boldsymbol{\sigma}\cdot(\mathbf{q}\times\mathbf{k}) + \frac{1}{10}\left(g_{v1} + \frac{1}{4}g_{v2}\right)i\boldsymbol{\sigma}\cdot(\mathbf{A}_{\rm out}\times\mathbf{A}_{\rm in})\left(\frac{|\mathbf{k}||\mathbf{q}|}{3\alpha^2}\right)^2, \tag{42}$$

$$\mathcal{O}_2(F) = \left(g_{s1} + \frac{1}{4}g_{s2}\right)\frac{1}{2}|\mathbf{A}_{\rm out}||\mathbf{A}_{\rm in}|\left(\cos^3\theta - \frac{3}{5}\cos\theta\right)\times\left(\frac{|\mathbf{k}||\mathbf{q}|}{3\alpha^2}\right)^2 + \left(g_{v1} + \frac{1}{4}g_{v2}\right)i\boldsymbol{\sigma}\cdot(\mathbf{A}_{\rm out}\times\mathbf{A}_{\rm in}) \times\frac{1}{2}\left(\cos^2\theta - \frac{1}{5}\right)\left(\frac{|\mathbf{k}||\mathbf{q}|}{3\alpha^2}\right)^2. \tag{43}$$

Then, using Eqs. (37) and (38) again, we can separate out the partial amplitudes $\mathcal{O}_n(l)$ for the states with different J^P in the same l as well. For example, we can separate out the resonance amplitudes with $J^p = 3/2^-$ [i.e., $\mathcal{O}_1(D_{I3})$] and $J^p = 5/2^-$ [i.e., $\mathcal{O}_1(D_{I5})$] from the amplitude $\mathcal{O}_1(D)$.

Finally, we should separate out the partial amplitudes with the same quantum numbers n, l, J^P in the different representations of the constituent quark model. We notice that the resonance transition strengths in the spin-flavor space are determined by the matrix element $\langle N_f|H_m^f|N_j\rangle\langle N_j|H_m^i|N_i\rangle$. Their relative strengths g_R ($R \equiv l_{I2J}[N_6, {}^{2S+1}N_3, \mathbf{L}]$) can be explicitly determined by the following relation:

$$\frac{g_{l_{I2J}[N_6,{}^{2S+1}N_3,L]}}{g_{l_{I2J}[N_6',{}^{2S'+1}N_3',L']}} = \frac{\langle N_f|I_3^f\sigma_{3z}|l_{I2J}[N_6,{}^{2S+1}N_3,L]\rangle}{\langle N_f|I_3^f\sigma_{3z}|l_{I2J}[N_6',{}^{2S'+1}N_3',L']\rangle} \times\frac{\langle l_{I2J}[N_6,{}^{2S+1}N_3,L]|I_3^i\sigma_{3z}|N_i\rangle}{\langle l_{I2J}[N_6',{}^{2S'+1}N_3',L']|I_3^i\sigma_{3z}|N_i\rangle}, \tag{44}$$

At last, we obtain the single-resonance-excitation amplitudes $\mathcal{O}_R$ by the relation:

$$\mathcal{O}(n,l,J) = \sum_R \mathcal{O}_R(n,l,J) = \sum_R g_R\mathcal{O}(n,l,J). \tag{45}$$

In this work, the values of g_R for the reactions $K^-p \to \Sigma^0\pi^0$, $\Lambda\pi^0$, and $\bar{K}^0n$ have been derived in the symmetric quark model, which have been listed in Table II.

Taking into account the width effects of the resonances, the resonance transition amplitudes of the s channel can be generally expressed as [87,89]

$$\mathcal{M}_R^s = \frac{2M_R}{s - M_R^2 + iM_R\Gamma_R(\mathbf{q})}\mathcal{O}_R e^{-(\mathbf{k}^2+\mathbf{q}^2)/6\alpha^2}, \tag{46}$$

where $\Gamma_R(\mathbf{q})$ is an energy-dependent width introduced for the resonances in order to take into account the off-mass-shell effects in the reaction. It is adopted as [81,85,87]

$$\Gamma_R(\mathbf{q}) = \Gamma_R\frac{\sqrt{s}}{M_R}\sum_i x_i\left(\frac{|\mathbf{q}_i|}{|\mathbf{q}_i^R|}\right)^{2l+1}\frac{D(\mathbf{q}_i)}{D(\mathbf{q}_i^R)}, \tag{47}$$

where $|\mathbf{q}_i^R| = ((M_R^2 - M_b^2 + m_i^2)/4M_R^2 - m_i^2)^{1/2}$, and $|\mathbf{q}_i| = ((s - M_b^2 + m_i^2)/4s - m_i^2)^{1/2}$; x_i is the branching ratio of the resonance decaying into a meson with mass m_i and a baryon with mass M_b, and Γ_R is the total decay width of the resonance with mass M_R. $D(\mathbf{q}) = e^{-\mathbf{q}^2/3\alpha^2}$ is a fission barrier function.

TABLE III. The strength parameters C_R determined by the experimental data.

Parameter	$K^-p \to \Sigma^0\pi^0$	$K^-p \to \Lambda\pi^0$	$K^-p \to \bar{K}^0n$
$C^{[70,{}^2 1]}_{S_{01}(1405)}$	$1.13^{+0.17}_{-0.05}$	–	$0.72^{+0.03}_{-0.06}$
$C^{[70,{}^2 8]}_{S_{01}(1670)}$	$0.33^{+0.05}_{-0.08}$	–	$0.08^{+0.02}_{-0.03}$
$C^{[70,{}^2 8]}_{S_{11}(1630)}$	–	1.00	1.00
$C^{[70,{}^4 8]}_{S_{11}(1750)}$	–	$0.86^{+0.08}_{-0.12}$	$0.50^{+0.15}_{-0.15}$
$C^{[70,{}^2 10]}_{S_{11}(1810)}$	–	1.00	1.00
$C^{[70,{}^2 1]}_{D_{03}(1520)}$	$2.49^{+0.06}_{-0.05}$	–	$2.87^{+0.15}_{-0.15}$
$C^{[70,{}^2 8]}_{D_{03}(1690)}$	1.00	–	$0.30^{+0.08}_{-0.04}$
$C^{[70,{}^2 8]}_{D_{13}(1670)}$	–	1.00	$5.00^{+1.00}_{-2.00}$
$C^{[70,{}^4 8]}_{D_{13}(1740)}$	–	1.00	1.00
$C^{[70,{}^2 10]}_{D_{13}(1780)}$	–	1.00	1.00
$C^{[70,{}^4 8]}_{D_{15}(1775)}$	–	$0.78^{+0.20}_{-0.13}$	1.00
C_u	$0.68^{+0.05}_{-0.08}$	$0.95^{+0.03}_{-0.02}$	–
$\sqrt{\delta_{m_i}\delta_{m_f}}$	0.99 ± 0.01	1.13 ± 0.01	1.08 ± 0.01

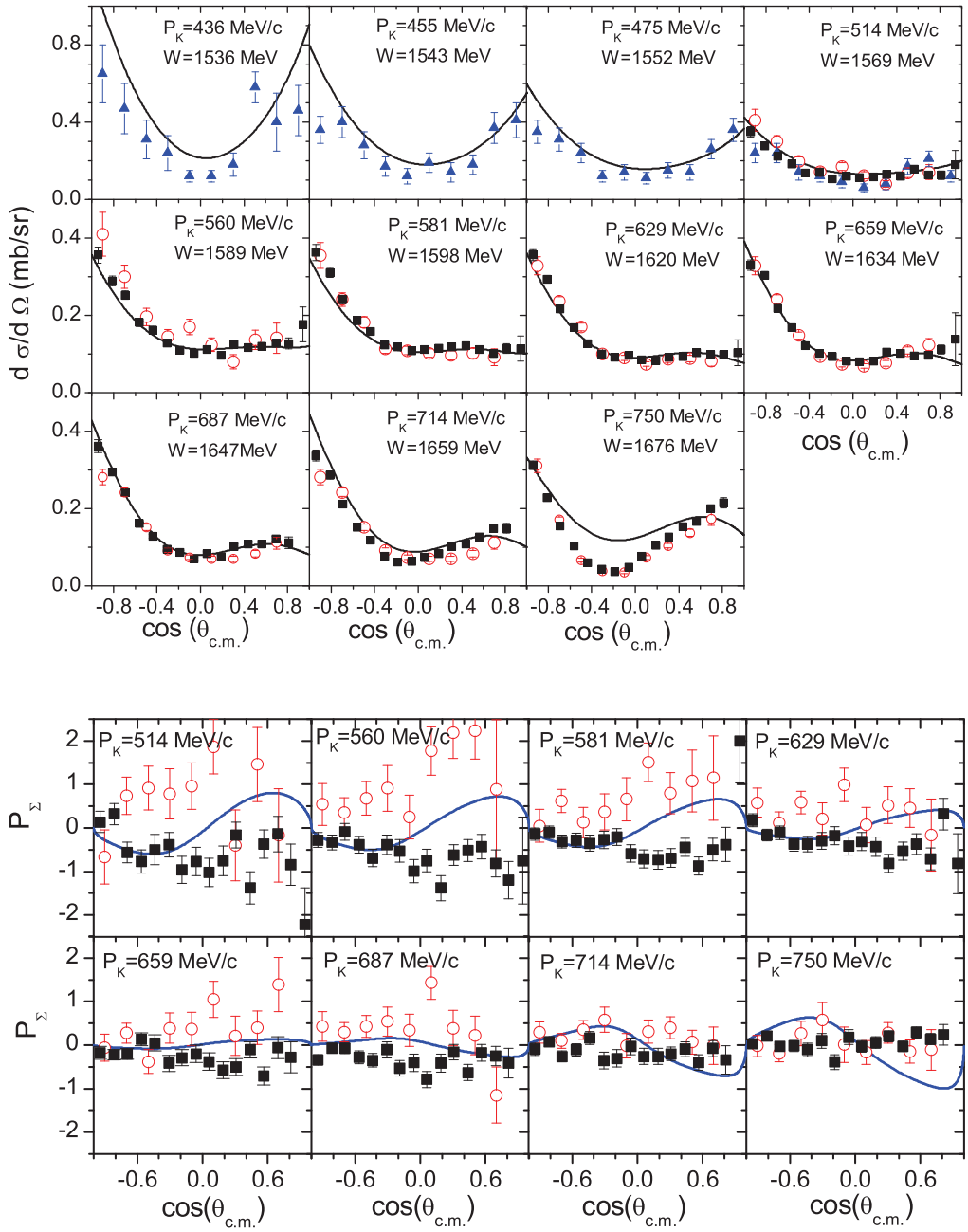

FIG. 2. (Color online) Differential cross sections (upper panel) and Σ^0 polarizations (lower panel) of the $K^- p \to \Sigma^0 \pi^0$ process compared with the data are from [76] (open circles), [77] (squares), and [57] (triangles).

IV. CALCULATION AND ANALYSIS

A. Parameters

With the transition amplitudes derived from the previous section, the differential cross section and polarization of final baryon can be calculated by

$$\frac{d\sigma}{d\Omega} = \frac{(E_i + M_i)(E_f + M_f)}{64\pi^2 s(2M_i)(2M_f)} \frac{|\mathbf{q}|}{|\mathbf{k}|} \frac{M_N^2}{2} \times \sum_{\lambda_i,\lambda_f} \left| \left[\frac{\delta_{m_i}}{f_{m_i}} \frac{\delta_{m_f}}{f_{m_f}} (\mathcal{M}_s + \mathcal{M}_u) + \mathcal{M}_t \right]_{\lambda_f,\lambda_i} \right|^2, \quad (48)$$

$$P = 2\frac{\mathrm{Im}[f(\theta)g^*(\theta)]}{|f(\theta)|^2 + |g(\theta)|^2}, \quad (49)$$

where $\lambda_i = \pm 1/2$ and $\lambda_f = \pm 1/2$ are the helicities of the initial and final state baryons, respectively. $\delta_{m_i}\delta_{m_f}$ is a global parameter accounting for the flavor symmetry-breaking effects arising from the quark-meson couplings, which is to be determined by experimental data. f_{m_i} and f_{m_f} are the initial and final meson decay constants, respectively.

In the calculation, the universal value of the harmonic oscillator parameter $\alpha = 0.4$ GeV is adopted. The masses of the u, d, and s constituent quarks are set as $m_u = m_d = 330$ MeV,

TABLE IV. Breit-Wigner masses M_R (MeV) and widths Γ_R(MeV) for the resonances.

$[N_6, {}^{2S+1}N_3, n, \mathbf{L}]$	$l_{I,2J}$	M_R	Γ_R	M_R (PDG)	Γ_R (PDG)
[**70**,^{2} 1, 1, **1**]	S_{01}	1410	80	1406 ± 4	50 ± 2
	D_{03}	1519	19	1520 ± 1	16 ± 1
[**70**,^{2} 10, 1, **1**]	S_{11}	1810	200	. . .	. . .
	D_{13}	1780	150	. . .	. . .
[**70**,^{2} 8, 1, **1**]	S_{01}	1674	50	1670 ± 10	$25 \sim 50$
	D_{03}	1685	62	1690 ± 5	60 ± 10
	S_{11}	1631	102	1620	$10 \sim 110$
	D_{13}	1674	52	1675 ± 10	60 ± 20
[**70**,^{4} 8, 1, **1**]	S_{11}	1770	90	1765 ± 35	$60 \sim 160$
	D_{13}	1740	80	. . .	. . .
	D_{15}	1775	105	1775 ± 5	120 ± 15
[**56**,^{2} 8, 2, **0**]	P_{01}	1600	150	1630 ± 70	150 ± 100
	P_{11}	1660	160	1660 ± 30	$40 \sim 200$

and $m_s = 450$ MeV, respectively. The decay constants for π and K are adopted as $f_\pi = 132$ MeV and $f_K = 160$ MeV, respectively.

In our framework, the resonance transition amplitude $\mathcal{O}_R$ is derived in the SU(6)⊗O(3) symmetric quark model limit. In reality, the SU(6)⊗O(3) symmetry is generally broken due to, e.g., spin-dependent forces in the quark-quark interaction. As a consequence, configuration mixings would occur, and an analytic solution cannot be achieved. To take into account the breaking of that symmetry, an empirical way [83,84] is to introduce a set of coupling strength parameters, C_R, for each resonance amplitude,

$$\mathcal{O}_R \to C_R \mathcal{O}_R, \tag{50}$$

where C_R should be determined by fitting the experimental observables. In the SU(6)⊗O(3) symmetry limit one finds $C_R = 1$, while deviations of C_R from unity imply the SU(6)⊗O(3) symmetry breaking. The determined values of C_R have been listed in Table III. For the uncertainties of the data, the parameters listed in Table III have some uncertainties as well. To know some uncertainties of a main parameter, we vary it around its central value until the predictions are inconsistent with the data within their uncertainties. The obtained uncertainties for the main parameters have been given in Table III as well.

In the t channel, two coupling constants, $G_V a$ from vector exchange and $g_{\rm SPP} g_{Sqq}$ from scalar exchange, are considered as free parameters. By fitting the data, we found that $G_V a \simeq 4$ and $g_{\rm SPP} g_{Sqq} \simeq 117$ for the $K^- p \to \Sigma^0\pi^0, \Lambda\pi^0, n\bar{K}^0$ processes.

In the calculations, the $n = 2$ shell $S = -1$ resonances in the s channel are treated as degeneration, and their degenerate mass and width are taken as $M = 1800$ MeV and $\Gamma = 100$ MeV, since in the low-energy region the contributions from the $n = 2$ shell are not significant. In the u channel, the intermediate states are the nucleon and its resonances. It is found that contributions from the $n \geqslant 1$ shells of the u channel are negligibly small, thus, the masses of the intermediate states for these shells are also treated as degeneration. In this work, we take $M_1 = 1650$ MeV ($M_2 = 1750$ MeV) for the degenerate mass of the $n = 1$ ($n = 2$) shell nucleon resonances. By fitting the data, we obtain the masses and widths of the main strange resonances in the s channel, which are listed in Table IV. Our results show that the resonance parameters are in agreement with the PDG values.

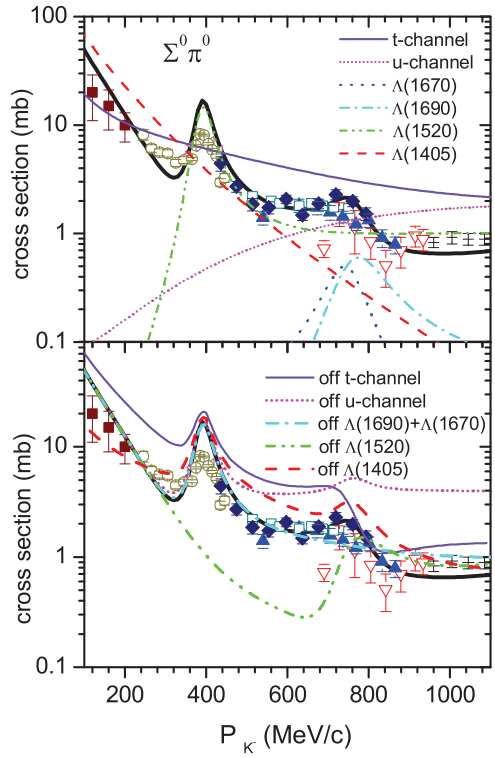

FIG. 3. (Color online) Cross section of the $K^- p \to \Sigma^0\pi^0$ process. The bold solid curves are for the full model calculations. Data are from Refs. [71] (down-triangles), [61] (solid circles), [57] (solid diamonds), [60] (left-triangles), [59] (up-triangles), [76] (open squares), and [67] (solid squares). In the upper panel, exclusive cross sections for $\Lambda(1405)S_{01}$, $\Lambda(1520)D_{03}$, $\Lambda(1670)S_{01}$, $\Lambda(1690)D_{03}$, t channel, and u channel are indicated explicitly by the legends in the figures. In the lower panel, the results by switching off the contributions of $\Lambda(1405)S_{01}$, $\Lambda(1520)D_{03}$, $\Lambda(1670)S_{01}$, $\Lambda(1690)D_{03}$, t channel, and u channel are indicated explicitly by the legends in the figures.

B. $K^- p \to \Sigma^0\pi^0$

The $K^- p \to \Sigma^0\pi^0$ process provides us a rather clear channel to study the Λ resonances, because only the Λ resonances contribute here for the isospin selection rule. The low-lying Λ resonances classified in the quark model are listed in Table I, from which we see that in $n = 0$ shell, only the Λ pole contributes to the process. In the $n = 1$ shell, two S-wave states (i.e., $[70,^2 8]\Lambda(1670)S_{01}$, $[70,^2 1]\Lambda(1405)S_{01}$), and two D-wave states (i.e., $[70,^2 1]\Lambda(1520)D_{03}$, $[70,^2 8]\Lambda(1690)D_{03}$) contribute to the reaction. The excitations of $[70,^4 8]$ are forbidden for the Λ-selection rule [96–98]. In our previous work [42], we have studied the $K^- p \to \Sigma^0\pi^0$ process. For more accurate data of $K^- p \to \Sigma^0\pi^0$, $\bar{K}^0 n$ are reported recently, which can be used to further constrain the properties

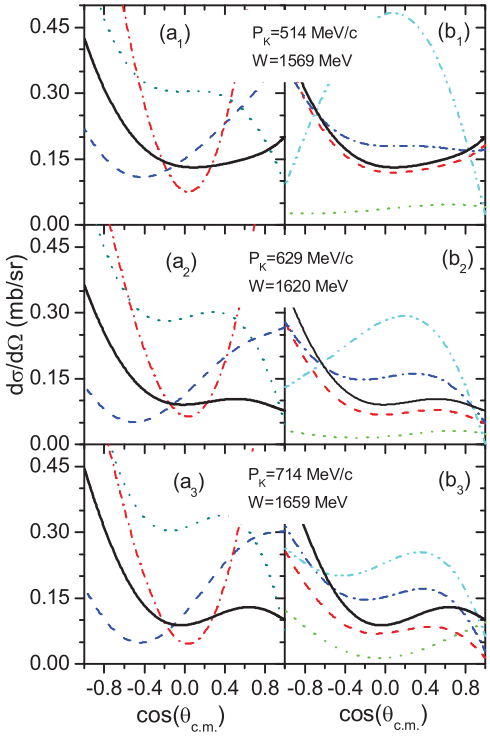

FIG. 4. (Color online) Effects of backgrounds and individual resonances on the differential cross sections at three energies for the $K^- p \to \Sigma^0 \pi^0$ process. The bold solid curves are for the full model calculations. In panels (a_1)–(a_3), the dashed, dotted, and dash-dotted are for the results given by switching off the contributions from the Λ pole, u channel and t channel, respectively. In panels (b_1)–(b_3), the dotted, dashed, dash-dotted, and dash-dot-dotted curves stand for the results given by switching off the contributions from $\Lambda(1520)D_{03}$, $\Lambda(1690)D_{03}$, $\Lambda(1670)S_{01}$, and $\Lambda(1405)S_{01}$, respectively.

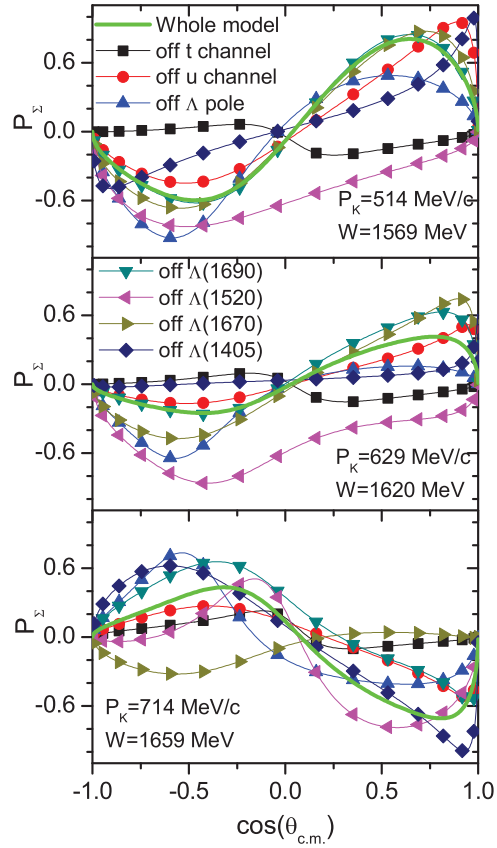

FIG. 5. (Color online) Effects of backgrounds and individual resonances on the Σ^0 polarizations at three energies for the $K^- p \to \Sigma^0 \pi^0$ process. The bold solid curves are for the full model calculations. The results by switching off the contributions from $\Lambda(1405)S_{01}$, $\Lambda(1670)S_{01}$, $\Lambda(1520)D_{03}$, $\Lambda(1690)D_{03}$, Λ pole, and u- and t-channel backgrounds are indicated explicitly by the legend.

of the Λ resonances. In this work we revisit the $K^- p \to \Sigma^0 \pi^0$ process. The differential cross sections, Σ^0 polarizations and total cross sections compared with the data are shown in Figs. 2 and 3. They are well described with the parameters determined by fitting the 112 data of the differential cross sections from Ref. [77]. The χ^2 per datum point is about $\chi^2/N = 3.4$. The main conclusions of our previous study [42] still hold as compared with those of the present work. In this work, the descriptions of the differential cross sections at forward angles are obviously improved (see Fig. 2). From Fig. 2, it is seen that the measurements of the Σ^0 polarizations from [76] and [77] are not consistent with each other. Our theoretical results of Σ^0 polarizations show some agreement with the measurements from [77] at backward angles.

Combining the determined C_R and g_R factors, we derive the ratios of the strengths ($\propto g_R C_R$) for the S- and D-wave resonances in the reaction, which are

$$\mathcal{G}_{S_{01}(1405)} : \mathcal{G}_{S_{01}(1670)} \simeq -9 : 1, \quad (51)$$

$$\mathcal{G}_{D_{03}(1520)} : \mathcal{G}_{D_{03}(1690)} \simeq -7 : 1. \quad (52)$$

From the ratios, it is found that the $\Lambda(1405)S_{01}$ and $\Lambda(1520)D_{03}$ govern the contributions of S and D waves, respectively, in the reaction. The reversed signs in the two S waves (D waves) indicates that they have destructive interferences each other.

It should be mentioned that our analysis suggests a much weaker contribution of $\Lambda(1670)S_{01}$ in the reaction than that derived from the symmetry quark model. The coupling strength parameter, C_R, is about 1/3 of that derived in the SU(6)⊗O(3) limit. The weaker contribution of $\Lambda(1670)S_{01}$ might be explained by the configuration mixing between $\Lambda(1405)S_{01}$ and $\Lambda(1670)S_{01}$ [42]. An *et al.* also predicted the existence of configuration mixings within the $\Lambda(1405)S_{01}$ and $\Lambda(1670)S_{01}$ by analyzing the decay properties of $\Lambda(1405)S_{01}$ [19]. On the other hand, to well describe the data, a large amplitude of $\Lambda(1520)D_{03}$ in the reaction is needed, which is about a factor of 2.5 larger than that derived in the SU(6)⊗O(3) limit (i.e., $C_{D_{03}(1520)} \simeq 2.5$). This means that we underestimate the couplings of $\Lambda(1520)D_{03}$ to $\bar{K}N$ and/or $\pi\Sigma$ in the SU(6)⊗O(3) limit for some reasons.

The dominant roles of $\Lambda(1405)S_{01}$ and $\Lambda(1520)D_{03}$ in the reaction can be obviously seen in the cross section, differential cross sections, and Σ^0 polarizations. Switching off the contribution of $\Lambda(1405)S_{01}$ or $\Lambda(1520)D_{03}$, the cross

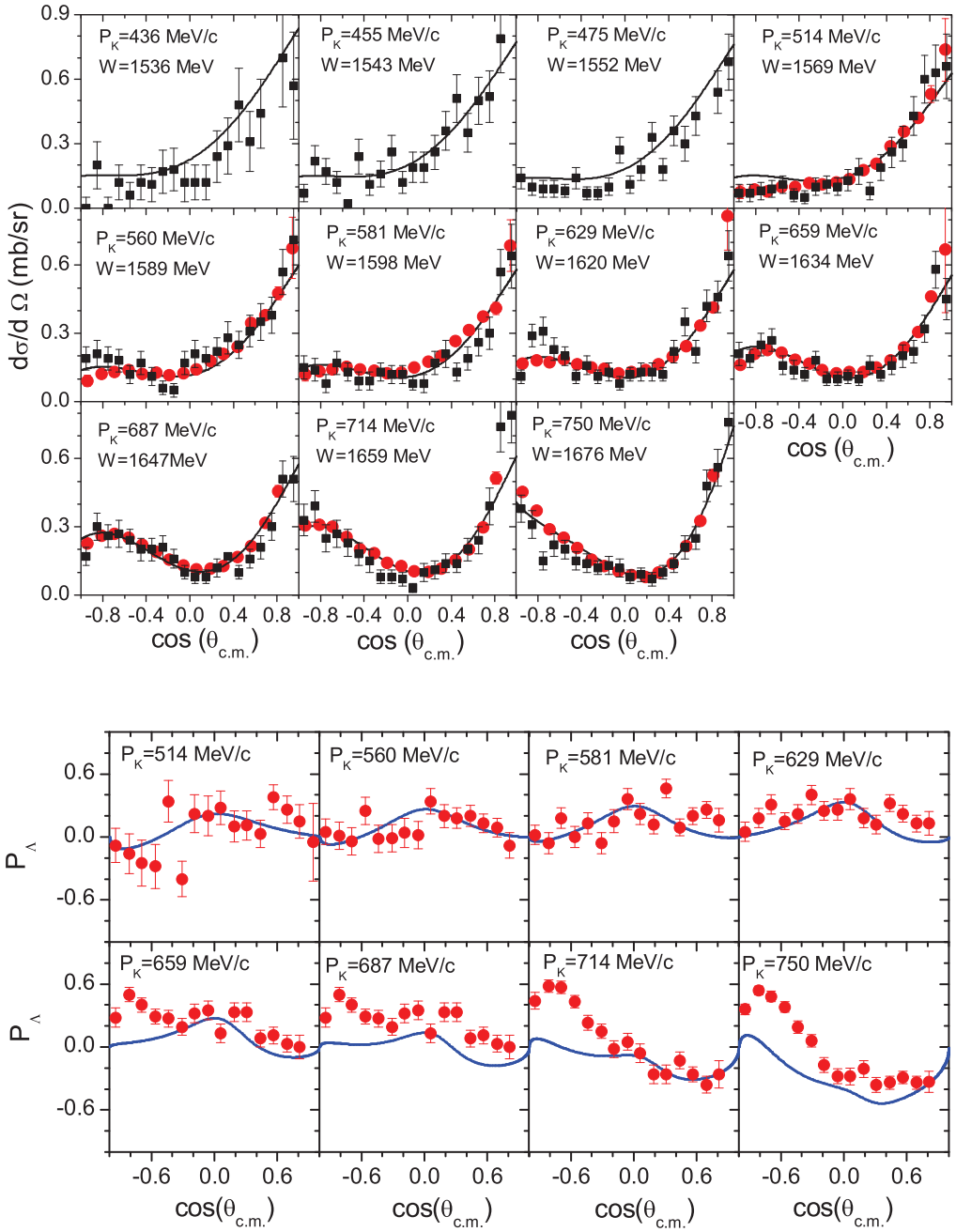

FIG. 6. (Color online) Differential cross sections (upper panel) and Λ polarizations (lower panel) of $K^- p \to \Lambda\pi^0$ compared with the data from [77] (solid circles) and [57] (squares).

section, differential cross sections, and polarizations change dramatically (see Figs. 3–5). The cross sections in the low-energy region $P_{K^-} \lesssim 300$ MeV/c ($W \lesssim 1.49$ GeV) are sensitive to the mass of $\Lambda(1405)S_{01}$. From Figs. 3 and 4 it is seen that $\Lambda(1520)D_{03}$ plays a crucial role in the low-energy region. Around $P_{K^-} = 400$ MeV/c ($W \simeq 1.52$ GeV), $\Lambda(1520)D_{03}$ is responsible for the sharp resonant peak in the total cross section. The tail of the partial cross section of $\Lambda(1520)D_{03}$ can extend to the low-energy region $P_{K^-} \sim 300$ MeV/c ($W \sim 1.49$ GeV), and to the higher energy region $P_{K^-} \sim 750$ MeV/c ($W \sim 1.68$ GeV), which is consistent with the analysis of [34].

Although the contributions of $\Lambda(1670)S_{01}$ and $\Lambda(1690)D_{03}$ are not as strong as those of $\Lambda(1405)S_{01}$ and $\Lambda(1520)D_{03}$, their roles can be seen around its threshold as well. If we switch off one of their contributions, the differential cross sections and Σ^0 polarizations change significantly at $P_{K^-} \simeq 700 \sim 800$ MeV/c ($W \simeq 1.65 \sim 1.7$ GeV) (see Figs. 4 and 5). From Fig. 3, it is found that the bump structure around $P_{K^-} = 780$ MeV/c ($W \simeq 1.69$ GeV) in the cross sections comes from the interferences between $\Lambda(1670)S_{01}$ and $\Lambda(1690)D_{03}$. Turning off the contributions of $\Lambda(1670)S_{01}$ and $\Lambda(1690)D_{03}$ at the same time, the bump structure around $P_{K^-} = 780$ MeV/c ($W \simeq 1.69$ GeV) will disappear.

Both u- and t-channel backgrounds play crucial roles in the reactions. Switching off the t-channel contribution, the differential cross sections are strongly overestimated at both forward and backward angles, while the sign of the polarization is even changed. The u-channel effects on the differential cross sections also can be obviously seen, if its contribution is switched off, and differential cross sections are overestimated significantly.

Finally, it should be pointed out that the Λ pole also plays an important role in the reaction. It has large effects on both the differential cross sections and Σ^0 polarizations in the whole energy region that we considered, although it has negligible effects on the total cross section. Switching off its contributions, the differential cross sections and Σ^0 polarizations are dramatically changed at both forward and backward angles (see Figs. 4 and 5).

As a whole, the resonances $\Lambda(1405)S_{01}$ and $\Lambda(1520)D_{03}$ play dominant roles in the reactions. Although the contributions of $\Lambda(1670)S_{01}$ and $\Lambda(1690)D_{03}$ are much weaker than those of $\Lambda(1405)S_{01}$ and $\Lambda(1520)D_{03}$, obvious evidence of $\Lambda(1670)S_{01}$ and $\Lambda(1690)D_{03}$ in the reaction can be seen around their threshold. The interferences between $\Lambda(1670)S_{01}$ and $\Lambda(1690)D_{03}$ might be responsible for the bump structure around $W = 1.69$ GeV in the cross section. There might exist configuration mixings between $\Lambda(1405)S_{01}$ and $\Lambda(1670)S_{01}$. The backgrounds also play crucial roles in the reactions. The differential cross sections are sensitive to the Λ pole, although the total cross section is less sensitive to it. The u- and t-channel backgrounds dramatically affect both the angle distributions and total cross section.

C. $K^- p \to \Lambda\pi^0$

In this reaction, the intermediate states of the s channel can only be hyperons with isospin $I = 1$ (i.e., Σ hyperons) for the isospin selection rule. Thus, this reaction provides us a rather clear place to study the Σ resonances. The low-lying Σ resonances classified in the quark model are listed in Table I. From the table, we see that in the $n = 0$ shell there are two P waves: $\Sigma(1193)P_{11}$ and $\Sigma(1385)P_{13}$. While in the $n = 1$ shell, there exist three S_{11} waves: $[70,^2 10]S_{11}$, $[70,^2 8]S_{11}$, and $[70,^4 8]S_{11}$; three D_{13} waves: $[70,^2 10]D_{13}$, $[70,^2 8]D_{13}$, and $[70,^4 8]D_{13}$; and one D_{15} wave: $[70,^4 8]D_{15}$. In these resonances only two states $\Sigma(1670)D_{13}$ and $\Sigma(1775)D_{15}$ are well established [1]. According to the classifications of the constituent quark model, they correspond to the representations $[70,^2 8, 1, \mathbf{1}]$ and $[70,^4 8, 1, \mathbf{1}]$, respectively. Although, many Σ resonances have been listed in the PDG book [1], their properties are still controversial. The Σ spectroscopy is far from being established. In the present work, we have carefully analyzed the new data of $K^- p \to \Lambda\pi^0$. Our results compared with the data have been shown in Figs. 6 and 7. From these figures, it is seen that the low-energy reaction $K^- p \to \Lambda\pi^0$ can be well described with the parameters (see Table III) determined by fitting 252 data points of the differential cross sections and Λ polarizations from Ref. [77], except some differences between theoretical results and the observations of the Λ polarizations in the higher energy region $P_{K^-} \gtrsim 650$ MeV/c ($W \gtrsim 1.63$ GeV). The χ^2 per datum point is about $\chi^2/N = 5.3$.

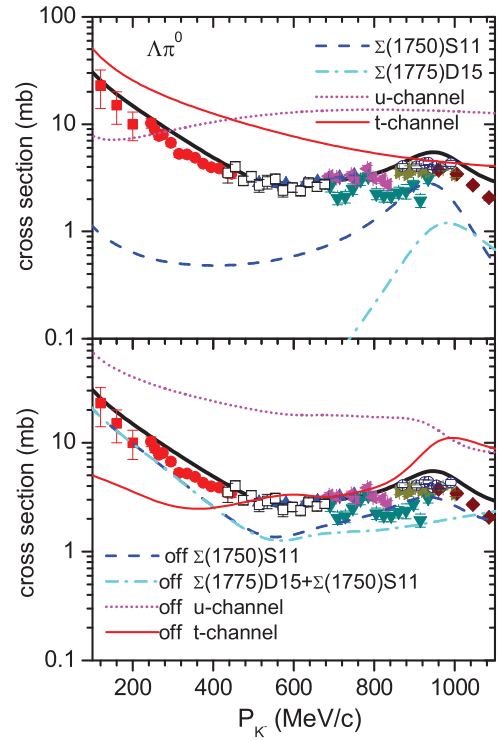

FIG. 7. (Color online) Cross section of the $K^- p \to \Lambda\pi^0$ process. The bold solid curves are for the full model calculations. Data are from Refs. [57] (open squares), [58] (solid circles), [70] (left-triangles), [66] (right-triangles), [71] (down-triangles), [77] (up-triangles), [63] (open circles), [67] (solid squares), and [69] (solid diamonds). In the upper panel, exclusive cross sections for $\Sigma(1750)$, $\Lambda(1775)$, t channel, and u channel are indicated explicitly by the legends in the figures. In the lower panel, the results by switching off the contributions of $\Sigma(1750)$, $\Lambda(1775)$, t channel, and u channel are indicated explicitly by the legends in the figures.

According to the determined g_R and C_R factors, we derive the strength ratios between the S-wave resonances, which are

$$\mathcal{G}_{S_{11}[70,^2 8]} : \mathcal{G}_{S_{11}[70,^4 8]} : \mathcal{G}_{S_{11}[70,^2 10]} \simeq -1 : 4 : -1. \quad (53)$$

It indicates the dominant contributions of $S_{11}[70,^4 8]$ in the S waves, while the derived strength ratios between the D_{13} waves are

$$\mathcal{G}_{D_{13}[70,^2 8]} : \mathcal{G}_{D_{13}[70,^4 8]} : \mathcal{G}_{D_{13}[70,^2 10]} \simeq 5 : -4 : -5. \quad (54)$$

It is shown that these D-wave resonances with $J^P = 3/2^-$ have comparable contributions to the reaction.

From Table I, it is found that the low-lying three S-wave resonances $[70,^2 10]S_{11}$, $[70,^2 8]S_{11}$, and $[70,^4 8]S_{11}$ are not established at all. According to the predictions of the traditional quark model, the masses of the S-wave Σ resonances should be larger than 1.6 GeV, however, the PDG has listed some states with mass less than 1.6 GeV, such as $\Sigma(1480)$, $\Sigma(1560)$, and $\Sigma(1580)$. We carefully analyze the differential cross sections, cross sections, and Λ polarizations of the reaction $K^- p \to \Lambda\pi^0$. We have found that the $[70,^4 8]S_{11}$ should have a mass of $\sim$1770 MeV, and a width of $\sim$90 MeV. This

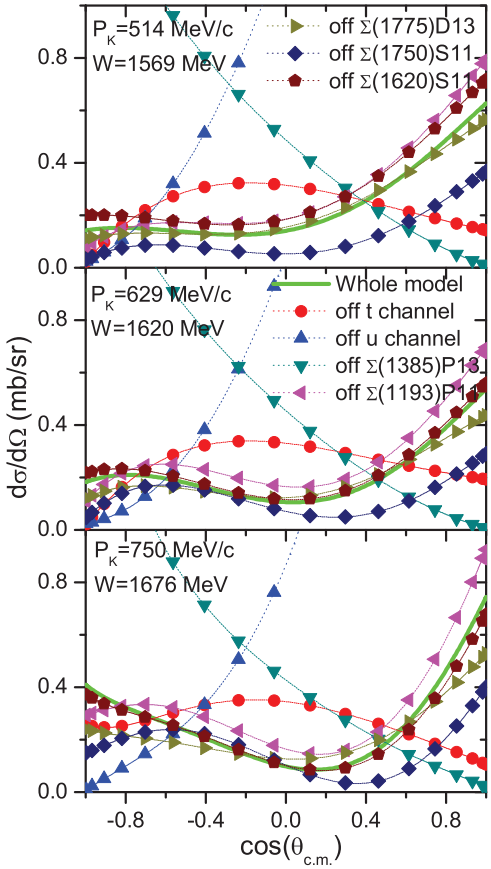

FIG. 8. (Color online) Effects of backgrounds and individual resonances on the differential cross sections at three energies for the $K^- p \to \Lambda\pi^0$ process. The bold solid curves are for the full model calculations. The results by switching off the contributions from $\Sigma(1193)$, $\Sigma(1385)$, $\Sigma(1620)$, $\Sigma(1750)$, $\Sigma(1775)$, and u- and t-channel backgrounds are indicated explicitly by the legend.

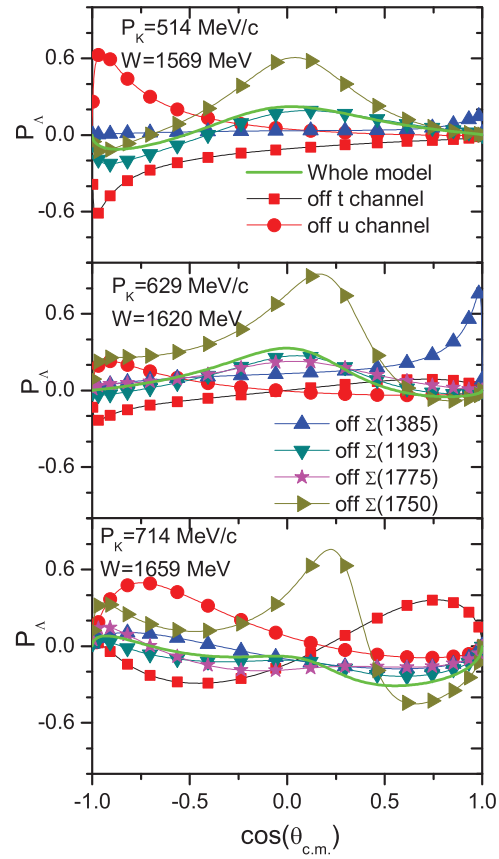

FIG. 9. (Color online) Effects of backgrounds and individual resonances on the Λ polarizations at three energies for the $K^- p \to \Lambda\pi^0$ process. The bold solid curves are for the full model calculations. The results by switching off the contributions from $\Sigma(1193)$, $\Sigma(1385)$, $\Sigma(1620)$, $\Sigma(1750)$, $\Sigma(1775)$, and the u- and t-channel backgrounds are indicated explicitly by the legend.

state has a significant contribution to the reaction in the whole resonance regions that we considered. Both the mass and width of this resonance are consistent with the three-star resonance $\Sigma(1750)1/2^-$ in PDG. Switching off its contributions, from Figs. 7–9 we find that the cross sections are obviously underestimated, and the shapes of the differential cross sections and polarizations change dramatically. Furthermore, we find that the resonance $[70,^2 8]S_{11}$ with a mass of $\sim$1631 MeV and a width of $\sim$100 MeV seems to be needed in the reactions, with which the descriptions of the data around $W \simeq 1.6$ GeV is improved slightly (see Fig. 8). This resonance is most likely to be the two-star state $\Sigma(1620)1/2^-$ in PDG. The quark model classifications for $\Sigma(1620)1/2^-$ and $\Sigma(1750)1/2^-$ suggested by us are consistent with the suggestions in Ref. [3]. It should be mentioned that no obvious evidence of $[70,^2 10]S_{11}$ is found in the reaction.

In the D waves, $\Sigma(1670)D_{13}$ and $\Sigma(1775)D_{15}$ are two well-established states. According to the quark model classifications, they correspond to the representations $[70,^2 8, 1, \mathbf{1}]$ and $[70,^4 8, 1, \mathbf{1}]$, respectively. Obvious roles of $\Sigma(1775)D_{15}$ can be found in the reaction. From Fig. 7, it is seen that the bump structure in the cross section around $P_{K^-} = 950$ MeV/c ($W \simeq 1.77$ GeV) is due to the interferences between $\Sigma(1775)D_{15}$ and $\Sigma(1750)S_{11}$. The effects of $\Sigma(1775)D_{15}$ on the differential cross sections can extend to the low-energy region $P_{K^-} \simeq 600$ MeV/c ($W \simeq 1.6$ GeV). Switching off the contribution of $\Sigma(1775)D_{15}$, one can see that the differential cross sections at very forward and backward angles change significantly. No confirmed evidence for $\Sigma(1670)D_{13}$ and the other D-wave resonances is found in the reaction.

It should be mentioned that the ground P-wave state $\Sigma(1385)P_{13}$ plays a crucial role in the reaction. Both the differential cross sections and the Λ polarizations are sensitive to it. Switching off the contributions of $\Sigma(1385)P_{13}$, one finds that the differential cross sections and Λ polarizations change dramatically (see Figs. 8 and 9). However, $\Sigma(1193)P_{11}$ has a small effect on the differential cross sections. Without $\Sigma(1193)P_{11}$, the differential cross sections only enhance slightly at forward angles.

$\Sigma(1660)P_{11}$ is a well-established state in the energy region what we considered, thus, we have analyzed its contributions to the reaction $K^- p \to \Lambda\pi^0$. It should be pointed out that we do not find any obvious evidence of $\Sigma(1660)P_{11}$ in the reaction. However, it should be mentioned that recently, Gao, Shi, and Zou had studied this reaction with an effective Lagrangian

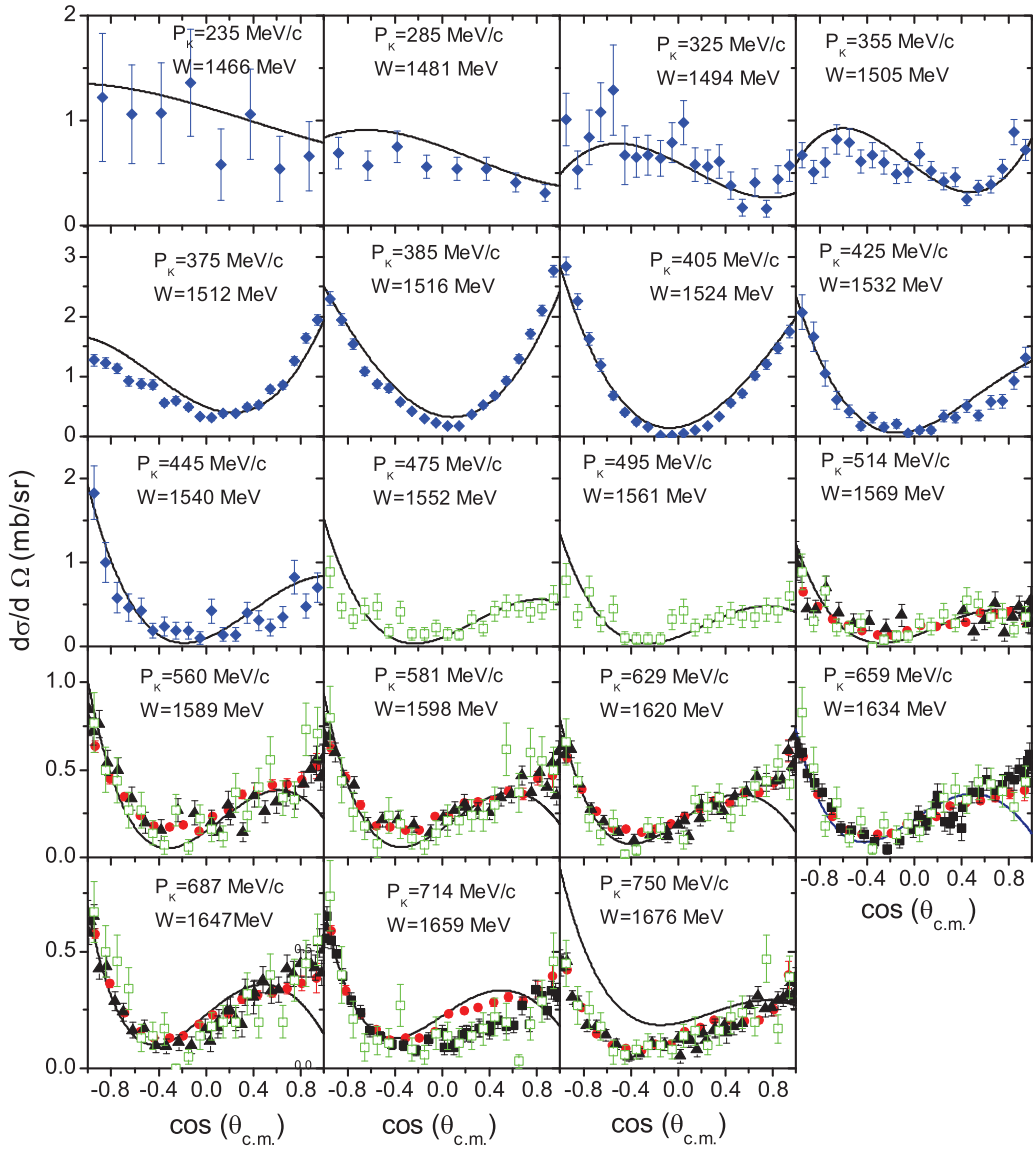

FIG. 10. (Color online) Differential cross sections of $K^- p \to \bar{K}^0 n$ compared with the data are from [58] (diamond), [77] (solid circles), [57] (open squares), and [64] (up-triangles).

approach as well; they claimed that their results clearly support the existence of $\Sigma(1660)P_{11}$ in the reaction [46].

Finally, it should be emphasized that the u- and t-channel backgrounds play dominant roles in the reaction. Both of the two channels not only are the main contributors to the total cross sections, but also have large effects on the differential cross sections and Λ polarizations (see Figs. 8 and 9).

In brief, the reaction $K^- p \to \Lambda\pi^0$ is dominated by the u- and t-channel backgrounds and the ground P-wave state $\Sigma(1385)P_{13}$. Furthermore, significant evidence of $\Sigma(1775)D_{15}$ and $\Sigma(1750)S_{11}$ can be found in the reaction. Some hints of $\Sigma(1620)1/2^-$ might exist in the reaction, with which the descriptions of the data around $W \simeq 1.6$ GeV is improved slightly. It should be pointed out that no confirmed evidence of the low mass resonances $\Sigma(1480)$, $\Sigma(1560)$, and $\Sigma(1580)$ listed in PDG is found in the $K^- p \to \Lambda\pi^0$ process.

D. $K^- p \to \bar{K}^0 n$

Both the isospin-1 and isospin-0 intermediate hyperons can contribute to the reaction $K^- p \to \bar{K}^0 n$. Thus, the properties of Λ and Σ resonances can be further constrained and/or confirmed by the study of the $K^- p \to \bar{K}^0 n$ process. We have analyzed the data of the low-energy reaction $K^- p \to \bar{K}^0 n$. Our results compared with the data are shown in Figs. 10 and 11. From these figures, it is found that the data are described fairly well within our chiral quark model. However, we also notice that our theoretical results might underestimate the differential cross sections at forward angles in the higher energy region $P_{K^-} \gtrsim 560$ MeV/c ($W \gtrsim 1.59$ GeV).

In the SU(6)⊗O(3) symmetry limit, the couplings of $\Lambda(1405)S_{01}$ and $\Lambda(1670)S_{01}$ to the $\bar{K}N$ should have the same value, however, the data favor a much weaker coupling of $\Lambda(1670)S_{01}$ to $\bar{K}N$ than that of $\Lambda(1405)S_{01}$, i.e.,

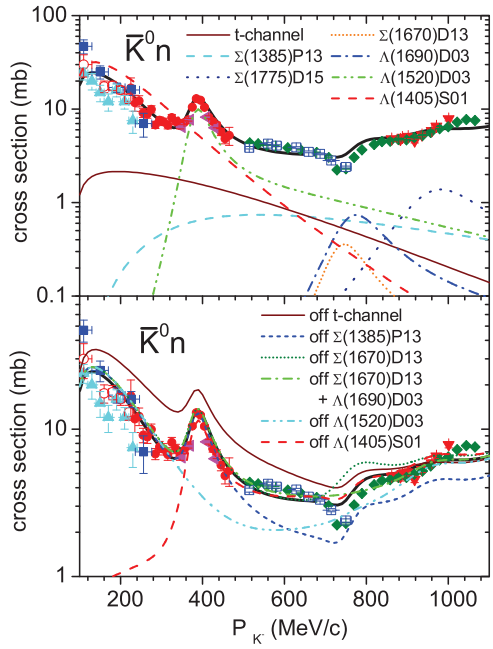

FIG. 11. (Color online) Cross section of the $K^-p \to \bar{K}^0n$ process. The bold solid curves are the full model calculations. Data are from Refs. [77] (open squares), [58] (solid circles), [60] (left-triangles), [66] (down-triangles), [65] (stars), [67] (up-triangles), [68] (open circles), and [62] (solid squares). In the upper panel, exclusive cross sections for $\Sigma(1385)$, $\Lambda(1405)$, $\Lambda(1520)$, $\Lambda(1690)$, $\Sigma(1670)$, $\Sigma(1775)$, and the t channel are indicated explicitly by the legends in the figures. In the lower panel, the results by switching off the contributions of $\Sigma(1385)$, $\Lambda(1405)$, $\Lambda(1520)$, $\Lambda(1690)$, $\Sigma(1670)$, $\Sigma(1775)$, and the t channel are indicated explicitly by the legends in the figures.

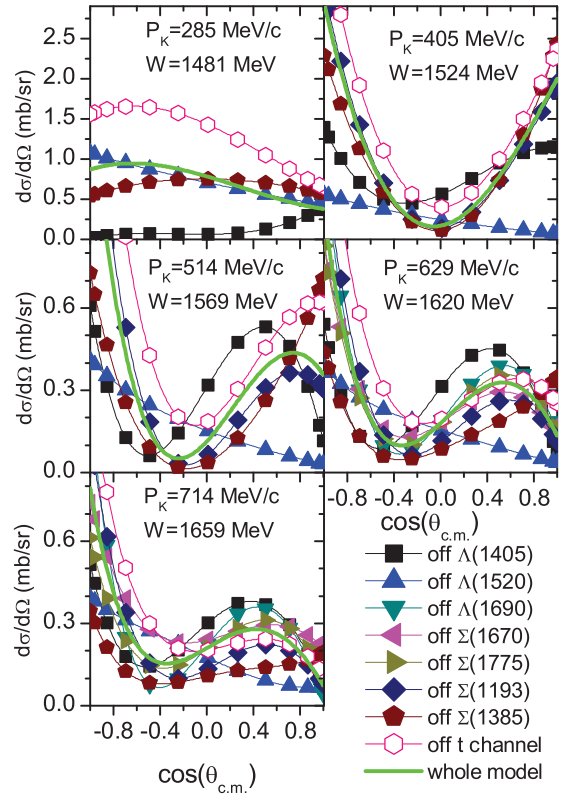

FIG. 12. (Color online) Effects of backgrounds and individual resonances on the differential cross sections at five energies for the $K^-p \to \bar{K}^0n$ process. The bold solid curves are for the full model calculations. The results by switching off the contributions from $\Sigma(1193)$, $\Sigma(1385)$, $\Sigma(1670)$, $\Sigma(1775)$, $\Lambda(1405)$, $\Lambda(1520)$, and t-channel backgrounds are indicated explicitly by the legend.

$|g_{\Lambda(1670)\bar{K}N}| \ll |g_{\Lambda(1405)\bar{K}N}|$, which consists with our previous analysis of the $K^-p \to \Sigma^0\pi^0$ process, where a very weak coupling of $\Lambda(1670)S_{01}$ to the $\bar{K}N$ is also needed. The weak coupling of $\Lambda(1670)S_{01}$ to $\bar{K}N$ was predicted with the UχPT approach as well [26]. The configuration mixing between $\Lambda(1670)S_{01}$ and $\Lambda(1405)S_{01}$ might explain the weak coupling of $\Lambda(1670)S_{01}$ to $\bar{K}N$ [42]. Furthermore, we find that the data favor a large coupling of $\Lambda(1520)D_{03}$ to $\bar{K}N$, which indicates that we might underestimate the coupling of $\Lambda(1520)D_{03}$ to $\bar{K}N$ in the SU(6)⊗O(3) limit. We also note that a larger coupling of $\Lambda(1520)D_{03}$ to $\bar{K}N$ is needed in the $K^-p \to \Sigma^0\pi^0$ process.

According to the determined C_R parameters and g_R factors, the ratios of the couplings of S-wave resonances to $\bar{K}N$ are obtained:

$$|g_{\Lambda(1405)\bar{K}N}| : |g_{\Lambda(1670)\bar{K}N}| : |g_{S_{11}[70,^28]\bar{K}N}| : |g_{S_{11}[70,^48]\bar{K}N}| : |g_{S_{11}[70,^210]\bar{K}N}| \simeq 5.2 : 1.9 : 1 : 2.5 : 1. \quad (55)$$

From the ratios, it is seen that $\Lambda(1405)S_{01}$ dominates the S-wave contributions in the reaction. For the D-wave resonances, the ratios of their couplings to $\bar{K}N$ are

$$|g_{\Lambda(1520)\bar{K}N}| : |g_{\Lambda(1690)\bar{K}N}| : |g_{\Sigma(1670)\bar{K}N}| : |g_{D_{13}[70,^48]\bar{K}N}| : |g_{D_{13}[70,^210]\bar{K}N}| \simeq 9 : 3 : 2 : 1. \quad (56)$$

It shows that $\Lambda(1520)D_{03}$ dominates D-wave contributions in the reaction.

Combing the ratios given in Eqs. (51)–(56), we can easily estimate some other important ratios:

$$\left|\frac{g_{\Lambda(1405)\Sigma\pi}}{g_{\Lambda(1670)\Sigma\pi}}\right| \simeq 3.8, \quad \left|\frac{g_{\Lambda(1520)\Sigma\pi}}{g_{\Lambda(1690)\Sigma\pi}}\right| \simeq 4.0. \quad (57)$$

In Figs. 11 and 12, we have shown the contributions of the main partial waves to the cross sections and differential cross sections in the reaction. From the figure, it is seen that $\Lambda(1405)S_{01}$ dominates the reaction at low energies. Switching off its contributions, we find that the cross sections at $P_{K^-} < 400$ MeV/c ($W < 1.52$ GeV) are dramatically underestimated (see Fig. 11). The differential cross sections are sensitive to $\Lambda(1405)S_{01}$ in the whole energy region that we considered, although it has less effects on the total cross sections at $P_{K^-} \gtrsim 400$ MeV/c ($W \gtrsim 1.52$ GeV).

The D-wave resonance $\Lambda(1520)D_{03}$ is crucial to the reaction as well. It is responsible for the sharp peak at $P_{K^-} \simeq 400$ MeV/c ($W \simeq 1.52$ GeV) in the cross section. The strong effects of $\Lambda(1520)D_{03}$ on the reaction can extend to the higher energy region $P_{K^-} \simeq 1000$ MeV/c ($W \simeq 1.79$ GeV). Switching off its contributions, the differential cross sections change dramatically in a wide energy region $P_{K^-} > 300$ MeV/c ($W > 1.49$ GeV). The bowl shape of the differential cross

section at $P_{K^-} \simeq 400$ MeV/c ($W \simeq 1.52$ GeV) is caused by the interferences between $\Lambda(1520)D_{03}$ and $\Lambda(1405)S_{01}$.

Furthermore, from Figs. 11 and 12, we can see slight effects of $\Lambda(1690)D_{03}$, $\Sigma(1670)D_{13}$, and $\Sigma(1775)D_{15}$ on the differential cross sections and cross sections in the energy region $P_{K^-} \gtrsim 600$ MeV/c ($W \gtrsim 1.6$ GeV). Their contributions to the cross section are much smaller than those of $\Lambda(1520)D_{03}$. The interferences between $\Lambda(1690)D_{03}$ and $\Sigma(1670)D_{13}$ might be responsible for the dip structure at $P_{K^-} \simeq 750$ MeV/c ($W \simeq 1.68$ GeV) in the cross section. If we switch off their contribution in the reaction, this dip structure will disappear (see Fig. 11).

In the s-channel ground states, it is seen that $\Sigma(1385)P_{13}$ plays an important role in the reaction. Without it, the cross sections in the region $P_K \gtrsim 500$ MeV/c ($W \gtrsim 1.56$ GeV) are obviously underestimated, and the differential cross sections are changed significantly. However, only a small contribution of $\Sigma(1193)P_{11}$ to the reaction is seen in the differential cross sections at $P_K \gtrsim 600$ MeV/c ($W \gtrsim 1.6$ GeV). Switching off it, the cross sections at forward angles should be slightly underestimated.

In the reaction $K^- p \to \bar{K}^0 n$, the t-channel background also plays a crucial role. Switching off it, we have noted that the cross sections are overestimated significantly, and the shapes of the differential cross sections change dramatically. The t channel has significant destructive interferences with $\Lambda(1405)S_{01}$.

It should be mentioned that in the $K^- p \to \bar{K}^0 n$ process, we do not find any confirmed evidence of $\Lambda(1670)S_{01}$, $\Sigma(1620)S_{11}$, $\Sigma(1750)S_{11}$, $\Lambda(1600)P_{01}$, and $\Sigma(1660)P_{11}$. Furthermore, we do not find any evidence of the low mass Σ resonances $\Sigma(1480)$, $\Sigma(1560)$, and $\Sigma(1580)$ listed in PDG.

Summarily, $\Lambda(1405)$ and $\Lambda(1520)D_{03}$ and t-channel background govern the $K^- p \to \bar{K}^0 n$ process at the low-energy regions. The ground P-wave state $\Sigma(1385)P_{13}$ also plays an important role in the reaction. Furthermore, some evidence of $\Lambda(1690)D_{03}$, $\Sigma(1670)D_{13}$, and $\Sigma(1775)D_{15}$ are seen in the reaction. The interferences between $\Lambda(1690)D_{03}$ and $\Sigma(1670)D_{13}$ might be responsible for the dip structure at $P_{K^-} \simeq 750$ MeV/c ($W \simeq 1.68$ GeV) in the cross section.

V. SUMMARY

In this work, we have carried out a combined study of the reactions $K^- p \to \Lambda\pi^0$, $\Sigma^0\pi^0$, and $\bar{K}^0 n$ in a chiral quark model. Good descriptions of the observations have been obtained at low energies. In these processes, the roles of the low-lying strangeness $S = -1$ hyperon resonances are carefully analyzed, and the properties of some hyperon resonances are derived.

By studying the $K^- p \to \Lambda\pi^0$ process, we find some significant evidence of the Σ resonance $[70,^4 8]S_{11}$. Both its mass and width are consistent with the three-star resonance $\Sigma(1750)1/2^-$ in PDG. Furthermore, we find that some hints of $[70,^2 8]S_{11}$ might exist in the reaction; its mass and width are consistent with the two-star resonance $\Sigma(1620)1/2^-$ in PDG. Obvious evidence of the D-wave resonance $\Sigma(1775)D_{15}$ is also found in the reaction. The bump structure in the cross sections around $W = 1.77$ GeV is due to the interferences between $\Sigma(1775)D_{15}$ and $\Sigma(1750)S_{11}$.

In the $K^- p \to \Sigma^0\pi^0$, $\bar{K}^0 n$ processes, both $\Lambda(1405)S_{01}$ and $\Lambda(1520)D_{03}$ play crucial roles. The observations of the two processes are sensitive to $\Lambda(1405)S_{01}$ and $\Lambda(1520)D_{03}$. $\Lambda(1520)D_{03}$ is responsible for the sharp peak in the cross sections around $P_{K^-} = 400$ MeV/c ($W \simeq 1.52$ GeV). $\Lambda(1520)D_{03}$ has a larger coupling to $\bar{K}N$ than that derived in the SU(6)⊗O(3) limit. Furthermore, in both of the processes $K^- p \to \Sigma^0\pi^0$ and $\bar{K}^0 n$, a weak coupling of $\Lambda(1670)S_{01}$ to $\bar{K}N$ is needed, which might be explained by the configuration mixing between $\Lambda(1670)S_{01}$ and $\Lambda(1405)S_{01}$.

Some evidence of $\Lambda(1670)S_{01}$ and $\Lambda(1690)D_{03}$ around their threshold is found in the $K^- p \to \Sigma^0\pi^0$ process. The interferences between $\Lambda(1670)S_{01}$ and $\Lambda(1690)D_{03}$ might be responsible for the bump structure around $W = 1.68$ GeV in the cross section.

Slight contributions from $\Lambda(1690)D_{03}$, $\Sigma(1670)D_{13}$, and $\Sigma(1775)D_{15}$ are found in the $K^- p \to \bar{K}^0 n$ process. The interferences between $\Lambda(1690)D_{03}$ and $\Sigma(1670)D_{13}$ might be responsible for the dip structure at $W \simeq 1.68$ GeV in the cross section.

The u- and t-channel backgrounds play crucial roles in the reactions $K^- p \to \Sigma^0\pi^0$, $\Lambda\pi^0$. The important role of the u channel in these reactions is also predicted with the BχPT [34] and UχPT approaches [21,30]. In $K^- p \to \bar{K}^0 n$, there are no u-channel contributions, while the t channel is crucial to give the correct shapes of the differential cross sections. The important role of the t channel is also found in the KN and πN processes [94].

The s-channel Born term plays an important role in the reactions. For the $K^- p \to \Lambda\pi^0$ process, both the differential cross sections and the Λ polarizations are sensitive to $\Sigma(1385)P_{13}$. For the $K^- p \to \Sigma^0\pi^0$ process, the Λ pole has large effects on the differential cross sections and Σ^0 polarizations in the whole energy region that we considered, although it has little effects on the total cross section. And for the $K^- p \to \bar{K}^0 n$ process, $\Sigma(1385)P_{13}$ has obvious effects on the cross sections and the differential cross sections.

It should be mentioned that no evidence of the low mass resonances $\Sigma(1480)$, $\Sigma(1560)$, and $\Sigma(1580)$ listed in PDG are found in the $K^- p \to \Lambda\pi^0$, $\Sigma^0\pi^0$, and $\bar{K}^0 n$ processes.

In this work we have only analyzed the $K^- p$ scattering to neutral final states. In our future work, we will carry out a systemical study of the reactions $K^- p$ scattering to charged final states, $K^- p \to \Sigma^\pm\pi^\mp$, $K^- p$. Of course, we expect high precision measurements of these reactions are to be performed at J-PARC in future experiments.

ACKNOWLEDGMENTS

This work is supported, in part, by the National Natural Science Foundation of China (Grants No. 11075051 and No. 11035006), Chinese Academy of Sciences (KJCX2-EW-N01), Program for Changjiang Scholars and Innovative Research Team in University (PCSIRT, Grant No. IRT0964), the Program Excellent Talent Hunan Normal University, and the Hunan Provincial Natural Science Foundation (Grants No. 11JJ7001 and No. 13JJ1018).

[1] J. Beringer *et al*. (Particle Data Group), Phys. Rev. D **86**, 010001 (2012).
[2] Y. Chen and B.-Q. Ma, Nucl. Phys. A **831**, 1 (2009).
[3] E. Klempt and J.-M. Richard, Rev. Mod. Phys. **82**, 1095 (2010).
[4] T. Melde, W. Plessas, and B. Sengl, Phys. Rev. D **77**, 114002 (2008).
[5] N. Isgur and G. Karl, Phys. Rev. D **18**, 4187 (1978).
[6] T. Melde and W. Plessas, Eur. Phys. J. A **35**, 329 (2008).
[7] N. Isgur and G. Karl, Phys. Lett. B **72**, 109 (1977); Phys. Rev. D **19**, 2653 (1979); **23**, 817(E) (1981); **20**, 1191 (1979).
[8] S. Capstick and N. Isgur, Phys. Rev. D **34**, 2809 (1986).
[9] S. M. Gerasyuta and E. E. Matskevich, Phys. Rev. D **76**, 116004 (2007).
[10] R. Bijker, F. Iachello, and A. Leviatan, Annals Phys. **284**, 89 (2000).
[11] L. Y. Glozman, W. Plessas, K. Varga, and R. F. Wagenbrunn, Phys. Rev. D **58**, 094030 (1998).
[12] U. Loring, B. C. Metsch, and H. R. Petry, Eur. Phys. J. A **10**, 447 (2001).
[13] C. L. Schat, J. L. Goity, and N. N. Scoccola, Phys. Rev. Lett. **88**, 102002 (2002).
[14] J. L. Goity, C. L. Schat, and N. N. Scoccola, Phys. Rev. D **66**, 114014 (2002).
[15] B. J. Menadue, W. Kamleh, D. B. Leinweber, and M. S. Mahbub, Phys. Rev. Lett. **108**, 112001 (2012).
[16] G. P. Engel, C. B. Lang, and A. Schafer, Phys. Rev. D **87**, 034502 (2013).
[17] R. Koniuk and N. Isgur, Phys. Rev. D **21**, 1868 (1980); **23**, 818(E) (1981).
[18] T. Melde, W. Plessas, and B. Sengl, Phys. Rev. C **76**, 025204 (2007).
[19] C. S. An, B. Saghai, S. G. Yuan, and J. He, Phys. Rev. C **81**, 045203 (2010).
[20] T. Hyodo and D. Jido, Prog. Part. Nucl. Phys. **67**, 55 (2012).
[21] J. A. Oller, J. Prades, and M. Verbeni, Phys. Rev. Lett. **95**, 172502 (2005).
[22] L. Roca, S. Sarkar, V. K. Magas, and E. Oset, Phys. Rev. C **73**, 045208 (2006).
[23] B. Borasoy, R. Nissler, and W. Weise, Eur. Phys. J. A **25**, 79 (2005).
[24] T. Hyodo, S. I. Nam, D. Jido, and A. Hosaka, Prog. Theor. Phys. **112**, 73 (2004).
[25] D. Jido, J. A. Oller, E. Oset, A. Ramos, and U. G. Meissner, Nucl. Phys. A **725**, 181 (2003).
[26] E. Oset, A. Ramos, and C. Bennhold, Phys. Lett. B **527**, 99 (2002); **530**, 260 (2002).
[27] C. Garcia-Recio, J. Nieves, E. R. Arriola, and M. J. Vicente Vacas, Phys. Rev. D **67**, 076009 (2003).
[28] J. A. Oller and U. G. Meissner, Phys. Lett. B **500**, 263 (2001); M. Mai and U.-G. Meissner, Nucl. Phys. A **900**, 51 (2013).
[29] E. Oset and A. Ramos, Nucl. Phys. A **635**, 99 (1998).
[30] J. A. Oller, Eur. Phys. J. A **28**, 63 (2006).
[31] J. A. Oller, J. Prades, and M. Verbeni, Eur. Phys. J. A **31**, 527 (2007).
[32] B. Borasoy, U. G. Meissner, and R. Nissler, Phys. Rev. C **74**, 055201 (2006).
[33] L. Roca, T. Hyodo, and D. Jido, Nucl. Phys. A **809**, 65 (2008).
[34] Antonio O. Bouzasa, Eur. Phys. J. A **37**, 201 (2008).
[35] A. D. Martin, N. M. Queen, and G. Violini, Nucl. Phys. B **10**, 481 (1969).
[36] D. M. Manley *et al*., Phys. Rev. Lett. **88**, 012002 (2001).
[37] M. F. M. Lutz and E. E. Kolomeitsev, Nucl. Phys. A **700**, 193 (2002).
[38] R. Buttgen, K. Holinde, and J. Speth, Phys. Lett. B **163**, 305 (1985).
[39] R. Buettgen, K. Holinde, A. Mueller-Groeling, J. Speth, and P. Wyborny, Nucl. Phys. A **506**, 586 (1990).
[40] A. Mueller-Groeling, K. Holinde, and J. Speth, Nucl. Phys. A **513**, 557 (1990).
[41] T. Hamaie, M. Arima, and K. Masutani, Nucl. Phys. A **591**, 675 (1995).
[42] X. H. Zhong and Q. Zhao, Phys. Rev. C **79**, 045202 (2009).
[43] A. D. Martin, Nucl. Phys. B **179**, 33 (1981).
[44] P. M. Gensini, R. Hurtado, and G. Violini, PiN Newslett. **13**, 291 (1997).
[45] J. J. Wu, S. Dulat, and B. S. Zou, Phys. Rev. D **80**, 017503 (2009).
[46] P. Gao, J. Shi, and B. S. Zou, Phys. Rev. C **86**, 025201 (2012).
[47] P. Gao, B. S. Zou, and A. Sibirtsev, Nucl. Phys. A **867**, 41 (2011).
[48] B.-C. Liu and J.-J. Xie, Phys. Rev. C **85**, 038201 (2012).
[49] A. Martinez Torres, K. P. Khemchandani, and E. Oset, Eur. Phys. J. A **35**, 295 (2008); Phys. Rev. C **77**, 042203 (2008).
[50] C. Garcia-Recio, M. F. M. Lutz, and J. Nieves, Phys. Lett. B **582**, 49 (2004).
[51] B. S. Zou, eConf C **070910**, 112 (2007), arXiv:0802.0087; Chin. Phys. C **33**, 1113 (2009).
[52] R. O. Bangerter, M. Alston-Garnjost, A. Barbaro-Galtieri, T. S. Mast, F. T. Solmitz, and R. D. Tripp, Phys. Rev. D **23**, 1484 (1981).
[53] A. Starostin *et al*. (Crystal Ball Collaboration), Phys. Rev. C **64**, 055205 (2001).
[54] S. Prakhov *et al*. (Crystall Ball Collaboration), Phys. Rev. C **70**, 034605 (2004).
[55] I. Zychor *et al*., Phys. Lett. B **660**, 167 (2008).
[56] J. Olmsted *et al*. (Crystal Ball Collaboration), Phys. Lett. B **588**, 29 (2004).
[57] R. Armenteros *et al*., Nucl. Phys. B **21**, 15 (1970).
[58] T. S. Mast, M. Alston-Garnjost, R. O. Bangerter, A. S. Barbaro-Galtieri, F. T. Solmitz, and R. D. Tripp, Phys. Rev. D **14**, 13 (1976).
[59] G. W. London *et al*., Nucl. Phys. B **85**, 289 (1975).
[60] D. Berley *et al*., Phys. Rev. D **1**, 1996 (1970); **3**, 2297(E) (1971).
[61] T. S. Mast, M. Alston-Garnjost, R. O. Bangerter, A. S. Barbaro-Galtieri, F. T. Solmitz, and R. D. Tripp, Phys. Rev. D **11**, 3078 (1975).
[62] J. Ciborowski *et al*., J. Phys. G **8**, 13 (1982).
[63] W. Cameron, B. Franek, G. P. Gopal, G. E. Kalmus, T. C. Bacon, I. Butterworth, and R. A. Stern, Nucl. Phys. B **193**, 21 (1981).
[64] M. Alston-Garnjost, R. W. Kenney, D. L. Pollard, R. R. Ross, R. D. Tripp, and H. Nicholson, Phys. Rev. D **17**, 2226 (1978).
[65] M. Alston-Garnjost, R. W. Kenney, D. L. Pollard, R. R. Ross, R. D. Tripp, H. Nicholson, and M. Ferro-Luzzi, Phys. Rev. D **17**, 2216 (1978); Phys. Rev. Lett. **38**, 1003 (1977).
[66] M. Jones, R. Levi Setti, D. Merrill, and R. D. Tripp, Nucl. Phys. B **90**, 349 (1975).
[67] J. K. Kim, Phys. Rev. Lett. **14**, 29 (1965); **19**, 1074 (1967); Columbia University, Report No. NEVIS-149 (1966).
[68] D. Evans, J. V. Major, E. Rondio, J. A. Zakrzewski, J. E. Conboy, D. J. Miller, and T. Tymieniecka, J. Phys. G **9**, 885 (1983).
[69] B. Conforto *et al*. (Rutherford-London Collaboration), Nucl. Phys. B **105**, 189 (1976).
[70] R. A. Ponte *et al*., Phys. Rev. D **12**, 2597 (1975).

[71] D. F. Baxter *et al*., Nucl. Phys. B **67**, 125 (1973).
[72] I. Zychor, Int. J. Mod. Phys. E **18**, 241 (2009).
[73] I. Zychor *et al*., Phys. Rev. Lett. **96**, 012002 (2006).
[74] M. Niiyama *et al*., Phys. Rev. C **78**, 035202 (2008).
[75] H. Kohri *et al*. (LEPS Collaboration), Phys. Rev. Lett. **104**, 172001 (2010).
[76] R. Manweiler *et al*., Phys. Rev. C **77**, 015205 (2008).
[77] S. Prakhov *et al*., Phys. Rev. C **80**, 025204 (2009).
[78] T. Abdullah and F. E. Close, Phys. Rev. D **5**, 2332 (1972).
[79] F. E. Close and Z. P. Li, Phys. Rev. D **42**, 2194 (1990).
[80] Q. Zhao, J. S. Al-Khalili, and C. Bennhold, Phys. Rev. C **64**, 052201(R) (2001).
[81] Q. Zhao, B. Saghai, and Z. P. Li, J. Phys. G **28**, 1293 (2002).
[82] Q. Zhao, Z. P. Li, and C. Bennhold, Phys. Rev. C **58**, 2393 (1998); Phys. Lett. B **436**, 42 (1998).
[83] J. He, B. Saghai, and Z. Li, Phys. Rev. C **78**, 035204 (2008).
[84] B. Saghai and Z. P. Li, Eur. Phys. J. A **11**, 217 (2001).
[85] Z. P. Li, Phys. Rev. D **48**, 3070 (1993); **50**, 5639 (1994); **52**, 4961 (1995); **52**, 1648 (1995).
[86] Z. P. Li, H. X. Ye, and M. H. Lu, Phys. Rev. C **56**, 1099 (1997).
[87] Q. Zhao, J. S. Al-Khalili, Z. P. Li, and R. L. Workman, Phys. Rev. C **65**, 065204 (2002).
[88] X.-H. Zhong and Q. Zhao, Phys. Rev. C **84**, 065204 (2011); **84**, 045207 (2011).
[89] X. H. Zhong, Q. Zhao, J. He, and B. Saghai, Phys. Rev. C **76**, 065205 (2007).
[90] X. H. Zhong and Q. Zhao, Phys. Rev. D **77**, 074008 (2008); **78**, 014029 (2008); **81**, 014031 (2010).
[91] X.-H. Zhong, Phys. Rev. D **82**, 114014 (2010).
[92] L.-H. Liu, L.-Y. Xiao, and X.-H. Zhong, Phys. Rev. D **86**, 034024 (2012).
[93] D. V. Bugg, A. V. Sarantsev, and B. S. Zou, Nucl. Phys. B **471**, 59 (1996); L. Li, B. S. Zou, and G. L. Li, Phys. Rev. D **67**, 034025 (2003); D. Lohse *et al*., Nucl. Phys. A **516**, 513 (1990); A. Bramon, A. Grau, and G. Pancheri, Phys. Lett. B **289**, 97 (1992); A. Bramon, R. Escribano, J. L. Lucio Martinez, and M. Napsuciale, *ibid*. **517**, 345 (2001); L. Roca, J. E. Palomar, E. Oset, and H. C. Chiang, Nucl. Phys. A **744**, 127 (2004); F. Klingl, N. Kaiser, and W. Weise, Z. Phys. A **356**, 193 (1996).
[94] F. Q. Wu and B. S. Zou, Chin. Phys. C **32**, 629 (2008).
[95] J. Hamilton and W. S. Woolcock, Rev. Mod. Phys. **35**, 737 (1963).
[96] Q. Zhao and F. E. Close, Phys. Rev. D **74**, 094014 (2006).
[97] N. Isgur, G. Karl, and R. Koniuk, Phys. Rev. Lett. **41**, 1269 (1978); **45**, 1738(E) (1980).
[98] A. J. G. Hey, P. J. Litchfield, and R. J. Cashmore, Nucl. Phys. B **95**, 516 (1975).